DSC 754

VOYAGER 1 & 2

CRS 8-HR CRUISE MODE

77-084A-08E /77-076A-08E

SPHE-00314 SPHE-00197

Table of Contents

1. Introduction

2. Errata/Change Log

3. LINKS TO RELEVANT INFORMATION IN THE ONLINE NSSDC INFORMATION SYSTEM

4. Catalog Materials

    a. Associated Documents

    b. Core Catalog Materials

---

1. INTRODUCTION:

The documentation for this data set was originally on paper, kept in NSSDC's Data Set Catalogs (DSCs). The paper documentation in the Data Set Catalogs have been made into digital images, and then collected into a single PDF file for each Data Set Catalog. The inventory information in these DSCs is current as of July 1, 2004. This inventory information is now no longer maintained in the DSCs, but is now managed in the inventory part of the NSSDC information system. The information existing in the DSCs is now not needed for locating the data files, but we did not remove that inventory information.

The offline tape datasets have now been migrated from the original magnetic tape to Archival Information Packages (AIP's).

A prior restoration may have been done on data sets, if a requestor of this data set has questions; they should send an inquiry to the request office to see if additional information exists.

2. ERRATA/CHANGE LOG:

NOTE: Changes are made in a text box, and will show up that way when displayed on screen with a PDF reader.

When printing, special settings may be required to make the text box appear on the printed output.

Version	Date	Person	Page	Description of Change
01				
02				

3 LINKS TO RELEVANT INFORMATION IN THE ONLINE NSSDC INFORMATION SYSTEM:

http://nssdc.gsfc.nasa.gov/nmc/

[NOTE: This link will take you to the main page of the NSSDC Master Catalog. There you will be able to perform searches to find additional information]

4. CATALOG MATERIALS:

a. Associated Documents To find associated documents you will need to know the document ID number and then click here. http://nssdcftp.gsfc.nasa.gov/miscellaneous/documents/

b. Core Catalog Materials

VOYAGER 1

VG1 CRS 6-HOUR CRUISE MODE DATA

77-084A-08B VG1 SPHE-00314

THIS DATA CONSISTS OF ONE CD. THE CD'REPLACE THE 9 TRACK TAPES. A DIRECTORY OF THE CD'S AS WELL A COPY OF THE REFERENCE DOCUMENT HAS BEEN PLACED IN THE CATALOG. THE KD WILL REPLACE THE DD & DC NUMBER,TIME SPAN AS FOLLOWS:

KD#	KW#	TIME-SPAN
KD022274	KW000178	09/7/77 – 06/30/05

VOYAGER 1

VG1 CRS 6-HOUR CRUISE MODE DATA

77-084A-08B

THIS DATA SET CONSISTS OF 3 MAGNETIC TAPES. THE TAPES ARE 9-TRACK, 6250 BPI, WRITTEN IN ASCII. THE TAPES WERE CREATED ON A VAX COMPUTER WITH A LABEL NAME OF "VG-CRS". A DIRECTORY OF THE TAPES, AS WELL AS A COPY OF THE REFERENCE DOCUMENT HAS BEEN INCLUDED IN THE CATALOG. THE D AND C NUMBERS ALONG WITH THE NUMBER OF FILES AND TIME SPANS ARE AS FOLLOWS:

D#	C#	FILES	TIME SPAN
D107993	C031719	19	09/07/77 - 12/31/93
D109110	C033107	45	09/07/77 - 12/31/90
D109111	C033108	27	01/01/91 - 12/31/98

Replaced

NSSDC Master Catalog Display
Experiment

Cosmic Ray System (CRS)

NSSDC ID: 77-084A-08
Mission Name: Voyager 1
Principal Investigator: Stone

Experiment mass: 7.50 kg
Average experiment power: 5.35 W

Description

This investigation studied the origin and acceleration process, life history, and dynamic contribution of interstellar cosmic rays, the nucleosynthesis of elements in cosmic-ray sources, the behavior of cosmic rays in the interplanetary medium, and the trapped planetary energetic-particle environment. The instrumentation included a High-Energy Telescope System (HETS) and a Low-Energy Telescope System (LETS). The HETS covered an energy range between 6 and 500 MeV/nucleon for nuclei ranging in atomic numbers from 1 through 30. In addition, electrons in the energy range between 3 and 100 MeV/nucleon were measured by this telescope and an electron telescope. The LETS measured the energy and determined the identity of nuclei for energies between 0.15 and 30 MeV/nucleon and atomic numbers from 1 to 30. The instruments also measured the anisotropies of electrons and nuclei. In addition, electrons in the energy range between 3 and 100 MeV/nucleon were measured by an electron telescope.

Discipline(s)

Astronomy/Cosmic Ray
Planetary Science/Fields and Particles
Space Physics/Heliospheric Studies

NSSDC Master Catalog Display
Experiment Personnel

Cosmic Ray System (CRS)

NSSDC ID: 77-084A-08

Principal Investigator

Prof. Edward C. Stone, Jr.
Mail Code 220-47
Downs Laboratory
California Institute of Technology
Pasadena, CA 91125

Electronic Mail
ECS@CITSRL.CALTECH.EDU (INTERNET)
HAMLET::ESTONE (NSI/DECNET)

Co-Investigator

Dr. Frank B. McDonald
Institute for Physical Science
and Technology
University of Maryland
College Park, MD 20742

Electronic Mail
SM27@UMAIL.UMD.EDU (INTERNET)
EAST::"SM27@UMAIL.UMD.EDU" (NSI/DECNET)

Dr. James H. Trainor
GSFC-Code 100

Dr. James H. Trainor
GSFC-Code 100

Prof. William R. Webber
Department of Astronomy
University of New Hampshire
Box 30001/ Dept 4500
Las Cruces, NM 88003-0001

Electronic Mail
BWEBBER@NMSU.EDU (INTERNET)

Prof. Jack R. Jokipii
Department of Planetary Sciences
University of Arizona
411 Space Science Building
Tucson, AZ 85721

Electronic Mail
JOKIPII@ARIZJVAX (BITNET)
JOKIPII@LPL.ARIZONA.EDU (INTERNET)
LOONEY::JOKIPII (NSI/DECNET)

NSSDC Contact

Dr. Edwin V. Bell, II
Hughes STX Corporation
Suite 400
7701 Greenbelt Road
Greenbelt, MD 20770

Electronic Mail
BELL@NSSDC (BITNET)
BELL@NSSDC.GSFC.NASA.GOV (INTERNET)
NSSDCA::BELL (NSI/DECNET)

Former Principal Investigator

Dr. Rochus E. Vogt
Department of Physics, Code 220-47
California Institute of Technology
Pasadena, CA 91125

NSSDC Master Catalog Display
Experiment Selected References

Cosmic Ray System (CRS)

NSSDC ID: 77-084A-08

1. Burlaga, L. F., McDonald, F. B., Goldstein, M. L., and Lazarus, A. J., Cosmic ray modulation and turbulent interaction regions near 11 au, J. Geophys. Res., 90, No. A12, 12027-12039, Dec. 1985.
2. Schardt, A. W., and Goertz, C. K., High-energy particles, In--Physics of the Jovian Magnetosphere, edited by A. J. Dessler, pp. 157--196, Cambridge U. Press., Cambridge, UK, 1983.
3. Schardt, A. W., and McDonald, F. B., Flux and source of energetic protons in Saturn's inner magnetosphere, J. Geophys. Res., 88, No. A11, 8923-8935, Nov. 1983.
4. Stone, E. C., Vogt, R. E., McDonald, F. B., Teegarden, B. J., Trainor, J. H., Jokipii, J. R., and Webber, W. R., Cosmic ray investigation for the Voyager missions; energetic particle studies in the outer heliosphere--and beyond, Space Sci. Rev., 12, No. 3, 355-376, Dec. 1977.
5. Vogt, R. E., Cook, W. R., Cummings, A. C., Garrard, T. L., Gehrels, N., Stone, E. C., Trainor, J. H., Schardt, A. W., Conlon, T., Lal, N., and McDonald, F. B., Voyager 1: Energetic ions and electrons in the Jovian magnetosphere, Science, 204, No. 4396, 1003-1006, June 1979.

For questions about this experiment, please contact:
Dr. Edwin V. Bell, II, bell@nssdc.gsfc.nasa.gov

For questions about the NSSDC's information systems, please contact:
Dr. James Thieman, thieman@nssdca.gsfc.nasa.gov, (301)286-9790
National Space Science Data Center, Code 633.2
NASA/Goddard Space Flight Center, Greenbelt, MD 20771

NASA Official: J. H. King, king@nssdca.gsfc.nasa.gov
Last Updated: 1996-03-08
Output Generated: 1997-01-12
Programming by: E. V. Bell, II

VOYAGER 2 COSMIC RAY (CRS) Experiment: SIX HOUR INTERPLANETARY COUNTING RATES AND FLUXES, 1977 - 2001

Principal Investigator: Prof. Edward C. Stone
Jet Propulsion Laboratory
California Institute of Technology

Data Contact: Dr. Nand Lal
Code 935
NASA Goddard Space Flight Center
Greenbelt, MD 20771
DECnet: LHEAVX::LAL
Internet: nand@voyager.gsfc.nasa.gov
Phone: 301-286-7350

Description: The SIX_HOUR subdirectory includes the full six-hour average interplanetary cruise count rate and flux data set in ASCII format from the Voyager 2 Cosmic Ray (CRS) experiment. The data set documentation in the VY2CRS_6H_FMT.txt file describes in detail the CRS experiment, processing of the data, and the format of this data set, and the VY2CRS_PUB.txt file gives a comprehensive list of publications from the CRS experiment team. Also see file VY2CRS_NMC.txt in the current directory for the experiment description from the NSSDC Master Catalog.

Data Source: NSSDC magnetic tape archive, data set 77-076A-08B

Related Information and Data:

Further details on the spacecraft, experiment, data sets at NSSDC, and related WWW sites can be found on the Voyager 1/2 flight project page under

http://nssdc.gsfc.nasa.gov/space/

Hour averages of the interplanetary solar wind data from, and hourly heliocentric coordinates of, Voyager 1/2 and other interplanetary spacecraft may be also be accessed and plotted on-line through the COHOWeb service based at the same WWW site as above.

Acknowledgement:

Use of these data in publications should be accompanied at minimum by acknowledgements of the National Space Science Data Center and the responsible Principal Investigator defined in the experiment documentation provided here.

C__DOCUME~1_bqueen_MYDOCU~1_VY1CRS~1[1]
File: VY1CRS_DIR.txt Version: NSSDC 02/04/2002 JFC

VOYAGER 1 COSMIC RAY (CRS) Experiment: SIX HOUR INTERPLANETARY COUNTING RATES AND FLUXES, 1977 - 2001

Principal Investigator: Prof. Edward C. Stone
Jet Propulsion Laboratory
California Institute of Technology

Data Contact: Dr. Nand Lal
Code 935
NASA Goddard Space Flight Center
Greenbelt, MD 20771
DECnet: LHEAVX::LAL
Internet: nand@voyager.gsfc.nasa.gov
Phone: 301-286-7350

Description: The SIX_HOUR subdirectory includes the full six-hour average interplanetary cruise count rate and flux data set in ASCII format from the Voyager 1 Cosmic Ray (CRS) experiment. The data set documentation in the VY1CRS_6H_FMT.txt file describes in detail the CRS experiment, processing of the data, and the format of this data set, and the VY1CRS_PUB.txt file gives a comprehensive list of publications from the CRS experiment team. Also see file VY1CRS_NMC.txt in the current directory for the experiment description from the NSSDC Master Catalog.

Data Source: NSSDC magnetic tape archive, data set 77-084A-08B

Related Information and Data:

Further details on the spacecraft, experiment, data sets at NSSDC, and related WWW sites can be found on the Voyager 1/2 flight project page under

http://nssdc.gsfc.nasa.gov/space/

Hour averages of the interplanetary solar wind data from, and hourly heliocentric coordinates of, Voyager 1/2 and other interplanetary spacecraft may be also be accessed and plotted on-line through the COHOWeb service based at the same WWW site as above.

Acknowledgement:

Use of these data in publications should be accompanied at minimum by acknowledgements of the National Space Science Data Center and the responsible Principal Investigator defined in the experiment documentation provided here.

NSSDC Master Catalog Display
Experiment

Cosmic Ray System (CRS)

NSSDC ID: 77-084A-08
Mission Name: Voyager 1
Principal Investigator: Stone

Experiment mass: 7.50 kg
Average experiment power: 5.35 W

Description

This investigation studied the origin and acceleration process, life history, and dynamic contribution of interstellar cosmic rays, the nucleosynthesis of elements in cosmic-ray sources, the behavior of cosmic rays in the interplanetary medium, and the trapped planetary energetic-particle environment. The instrumentation included a High-Energy Telescope System (HETS) and a Low-Energy Telescope System (LETS). The HETS covered an energy range between 6 and 500 MeV/nucleon for nuclei ranging in atomic numbers from 1 through 30. In addition, electrons in the energy range between 3 and 100 MeV/nucleon were measured by this telescope and an electron telescope. The LETS measured the energy and determined the identity of nuclei for energies between 0.15 and 30 MeV/nucleon and atomic numbers from 1 to 30. The instruments also measured the anisotropies of electrons and nuclei. In addition, electrons in the energy range between 3 and 100 MeV/nucleon were measured by an electron telescope.

Discipline(s)

Astronomy/Cosmic Ray
Planetary Science/Fields and Particles
Space Physics/Heliospheric Studies

NSSDC Master Catalog Display
Experiment Personnel

Cosmic Ray System (CRS)

NSSDC ID: 77-084A-08

Principal Investigator

Prof. Edward C. Stone, Jr.
Mail Code 220-47
Downs Laboratory
California Institute of Technology
Pasadena, CA 91125

Electronic Mail
ECS@CITSRL.CALTECH.EDU (INTERNET)
HAMLET::ESTONE (NSI/DECNET)

Co-Investigator

Dr. Frank B. McDonald
Institute for Physical Science
and Technology
University of Maryland
College Park, MD 20742

Electronic Mail
SM27@UMAIL.UMD.EDU (INTERNET)
EAST::"SM27@UMAIL.UMD.EDU" (NSI/DECNET)

Dr. James H. Trainor
GSFC-Code 100

Dr. James H. Trainor
GSFC-Code 100

Prof. William R. Webber
Department of Astronomy
University of New Hampshire
Box 30001/ Dept 4500
Las Cruces, NM 88003-0001

Electronic Mail
BWEBBER@NMSU.EDU (INTERNET)

Prof. Jack R. Jokipii
Department of Planetary Sciences
University of Arizona
411 Space Science Building
Tucson, AZ 85721

Electronic Mail
JOKIPII@ARIZJVAX (BITNET)
JOKIPII@LPL.ARIZONA.EDU (INTERNET)
LOONEY::JOKIPII (NSI/DECNET)

NSSDC Contact

Dr. Edwin V. Bell, II
Hughes STX Corporation
Suite 400
7701 Greenbelt Road
Greenbelt, MD 20770

Electronic Mail
BELL@NSSDC (BITNET)
BELL@NSSDC.GSFC.NASA.GOV (INTERNET)
NSSDCA::BELL (NSI/DECNET)

Former Principal Investigator

C__DOCUME~1_bqueen_MYDOCU~1_VY1CRS~2[1]

Dr. Rochus E. Vogt
Department of Physics, Code 220-47
California Institute of Technology
Pasadena, CA 91125

NSSDC Master Catalog Display
Experiment Selected References

Cosmic Ray System (CRS)

NSSDC ID: 77-084A-08

1. Burlaga, L. F., McDonald, F. B., Goldstein, M. L., and Lazarus, A. J., Cosmic ray modulation and turbulent interaction regions near 11 au, J. Geophys. Res., 90, No. A12, 12027-12039, Dec. 1985.
2. Schardt, A. W., and Goertz, C. K., High-energy particles, In--Physics of the Jovian Magnetosphere, edited by A. J. Dessler, pp. 157--196, Cambridge U. Press., Cambridge, UK, 1983.
3. Schardt, A. W., and McDonald, F. B., Flux and source of energetic protons in Saturn's inner magnetosphere, J. Geophys. Res., 88, No. A11, 8923-8935, Nov. 1983.
4. Stone, E. C., Vogt, R. E., McDonald, F. B., Teegarden, B. J., Trainor, J. H., Jokipii, J. R., and Webber, W. R., Cosmic ray investigation for the Voyager missions; energetic particle studies in the outer heliosphere--and beyond, Space Sci. Rev., 12, No. 3, 355-376, Dec. 1977.
5. Vogt, R. E., Cook, W. R., Cummings, A. C., Garrard, T. L., Gehrels, N., Stone, E. C., Trainor, J. H., Schardt, A. W., Conlon, T., Lal, N., and McDonald, F. B., Voyager 1: Energetic ions and electrons in the Jovian magnetosphere, Science, 204, No. 4396, 1003-1006, June 1979.

For questions about this experiment, please contact:
Dr. Edwin V. Bell, II, bell@nssdc.gsfc.nasa.gov

For questions about the NSSDC's information systems, please contact:
Dr. James Thieman, thieman@nssdca.gsfc.nasa.gov, (301)286-9790
National Space Science Data Center, Code 633.2
NASA/Goddard Space Flight Center, Greenbelt, MD 20771

NASA Official: J. H. King, king@nssdca.gsfc.nasa.gov
Last Updated: 1996-03-08
Output Generated: 1997-01-12
Programming by: E. V. Bell, II

Directory of VG1-CRS 6-HR CRUISE DATA

VY1HEADER.CRS;1	VY1CRS77.DAT;1	VY1CRS78.DAT;1	VY1CRS79.DAT;1
VY1CRS80.DAT;1	VY1CRS81.DAT;1	VY1CRS82.DAT;1	VY1CRS83.DAT;1
VY1CRS84.DAT;1	VY1CRS85.DAT;1	VY1CRS86.DAT;1	VY1CRS87.DAT;1
VY1CRS88.DAT;1	VY1CRS89.DAT;1	VY1CRS90.DAT;1	VY1CRS91.DAT;1
VY1CRS92.DAT;1	VY1CRS93.DAT;1	VY1CRS_REF.DOC;1	

Total of 19 files.

Header for NSSDC submission for Voyager-1 Cruise Archive
Applies to the TEXT datasets formed by program DCFLUX from the original BINARY IBM mainframe datasets.

VOL_CREATION_DATE: 1994-10-07

MEDIUM_DESCRIPTION: 1/2 inch, 9-track, 6250 bpi magnetic tape

TECHNICAL_CONTACT:
Dr. Nand Lal
Goddard Space Flight Center
Code 935
Greenbelt, MD 20771

Electronic Mail: LHEAVX::LAL
Electronic Mail: nand@voyager.gsfc.nasa.gov
Telephone: 301-286-7350

PREV_VOLS: None

DATA_SET_NAME: Voyager-1 Cruise Mode Data Archive

DATA_SOURCE: Voyager-1 Cosmic Ray Subsystem

SCIENTIFIC_CONTACT:
Dr. Frank McDonald
Institute for Physical Science and Technology
University of Maryland
College Park, MD 20742

Electronic Mail: fm27@umail.umd.edu
Telephone: 301-405-4861

SPACECRAFT_CHARACTERISTICS: Voyager-1 was launched on September 5, 1977, encountered Jupiter on March 5, 1979, and Saturn on November 12, 1980. After passing Saturn the spacecraft trajectory is taking it generally toward the nose of the terminator shock of the sun's heliosphere. At the end of 1992 it was about 50 AU from the sun, and above the ecliptic plane near 33 degrees N heliolatitude. The spacecraft is instrumented with a full suite of magnetic field, plasma and energetic particle and cosmic ray sensors. The Imaging experiment has sent back wonderful pictures of the planets and their moons and rings.

INVESTIGATION_OBJECTIVES: This instrument is designed to exploit to the fullest practical degree the proposed trajectories of Voyagers-1 and -2. The significance of these measurements will be greatly enhanced by concurrent measurements with similar particle telescopes on satellites such as the Pioneers, IMPs, and similar series in near-earth orbits. similar series in near-earth orbits. The principle scientific objectives of this experiment are:

more pages from the data

DSC # 754
77-084A-08B

Header for NSSDC submission for Voyager-1 Cruise Archive
Applies to the TEXT datasets formed by program DCFLUX from
the original BINARY IBM mainframe datasets.

VOL_CREATION_DATE: 1994-10-07

MEDIUM_DESCRIPTION: 1/2 inch, 9-track, 6250 bpi magnetic tape

TECHNICAL_CONTACT:
Dr. Nand Lal
Goddard Space Flight Center
Code 935
Greenbelt, MD 20771

Electronic Mail: LHEAVX::LAL
Electronic Mail: nand@voyager.gsfc.nasa.gov
Telephone: 301-286-7350

PREV_VOLS: None

DATA_SET_NAME: Voyager-1 Cruise Mode Data Archive

DATA_SOURCE: Voyager-1 Cosmic Ray Subsystem

SCIENTIFIC_CONTACT:
Dr. Frank McDonald
Institute for Physical Science and
Technology
University of Maryland
College Park, MD 20742

Electronic Mail: fm27@umail.umd.edu
Telephone: 301-405-4861

SPACECRAFT_CHARACTERISTICS: Voyager-1 was launched on September 5, 1977, encountered Jupiter on March 5, 1979, and Saturn on November 12, 1980. After passing Saturn the spacecraft trajectory is taking it generally toward the nose of the terminator shock of the sun's heliosphere. At the end of 1992 it was about 50 AU from the sun, and above the ecliptic plane near 33 degrees N heliolatitude. The spacecraft is instrumented with a full suite of magnetic field, plasma and energetic particle and cosmic ray sensors. The Imaging experiment has sent back wonderful pictures of the planets and their moons and rings.

INVESTIGATION_OBJECTIVES: This instrument is designed to exploit to the fullest practical degree the proposed trajectories of Voyagers-1 and -2. The significance of these measurements will be greatly enhanced by concurrent measurements with similar particle telescopes on satellites such as the Pioneers, IMPs, and similar series in near-earth orbits. similar series in near-earth orbits. The principle scientific objectives of this experiment are:

1.) To measure the flow patterns of energetic solar and galactic particles separately in the inter-planetary field. To interpret this measurement, simultaneous determination of the energy spectrum, radial gradient, distribution, and streaming parameters is required for each nuclear species and over as wide an energy range as is practicable.

2.) To measure the energy spectra, and isotopic composition of galactic and solar cosmic rays from the lowest practical energies up to ~800 MeV/nucleon and (by use of objective 1) to unfold the primary flare and interstellar spectrum.

3.) To measure the time variations of the differential energy spectra of electrons, hydrogen and helium nuclei over the corresponding energy intervals. During flare events, to obtain time histories; during quiet times, to relate gross time variations to those near earth thus deducing a spatial gradient for galactic cosmic rays.

4.) To study the energy spectra, time variations and spatial gradients associated with recurrent and non-flare associated interplanetary proton and helium streams and to define the related solar or inter-planetary acceleration processes.

5.) To provide information on the energetic particle distribution surrounding Jupiter and Saturn.

6.) To try to determine the extent of the solar cavity, the energetic particle phenomena occurring at this interface and the cosmic ray density in nearby interstellar space.

INSTRUMENT_ATTRIBUTES: The California Institute of Technology (CIT)/ Goddard Space Flight Center(GSFC) experiment on Voyager-1 and -2 (CRS) consists of three types of solid state detector telescopes, the High Energy Telescopes (HET-I and II), the Low Energy dE/dx vs. E Telescopes (LET A,B,C, and D) and The Electron Telescope (TET). The HETs and LETs are redundant and are designed to complement each other and to cover a broad range in energy, intensity, and charge spectra. Charged particle spectra are measured over energy intervals as follows:

Particle Component	Energy Range
Galactic cosmic ray protons and Solar protons	1.8 - 200 MeV
Galactic cosmic ray helium and Solar helium	1.8 - 500 MeV/nucleon
Galactic and Solar electrons	0.2- 13.0 MeV
Li,Be,B,C,N,O,F,Ne and their isotopic composition	6 MeV/nuc - 200 MeV/nuc
Integral flux of IONS > 70 MeV	

Geometrical Factors

HET Varies from about .74 - 1.7 depending if the event is A or B Stopping or

	Penetrating
LET	0.440 cm2-ster. (nominal)
TET	Varies from about .66 - 3.12 depending upon depth of penetration into the Di stack.

High Energy Telescope: The HET consists of a multi-element stack of solid state detectors. Particles can enter this telescope from both ends of this stack. The Two "A" elements (see diagram below) are single lithium drift detectors, 8 cm2 area and .15 mm thick. The "C1" element is a surface barrier detector 8 cm2 and 3 mm thick. Next is an array of six "C" surface barrier detectors each 8 cm2 and 6 mm thick and finally two curved 8 cm2 and 2 mm thick "B" detectors are stacked to form a two-ended telescope.

For particles which come to rest within this stack (4 - 70 MeV/ nucleon) three measurements are made: energy loss (dE/dx), total energy, and range. For particles which penetrate completely through the stack of solid state detectors three separate dE/dx measurements are made. This multiparameter analysis reduces the back-ground level of spurious events to a negligible level. Charge resolution for penetrating particles is possible up to about 200 MeV/nucleon. It is estimated that the absolute uncertainty in the helium flux is about 7% at 400 MeV and about 5% at energies below 200 MeV.

Low Energy Telescope. This detector was designed to measure low-energy solar flare particles in the interplanetary space and trapped particles in the Jovian and Saturnian magnetospheres. Its geometry factor (4.4E-01 cm**2.sr) allows measurement of fluxes as high as 5.0E+05/(cm**2.s.sr). The LET is a double dE/dx vs. E solid state detector. To enter this telescope a particle must pass through a 4 uM Aluminum collimator which helps define the geometry. Then two thin (35 microns thickness and 2.8 cm2 area) surface barrier detectors provide a double dE/dx measurement. Two thick (450 uM thickness and 4.5 cm2 area) lithium drift detectors provide another dE/dx and a total energy measurement. The LET covers the energy range 1.8 to 22 MeV/nucleon with charge resolution from Z=1 to 8.

The Electron Telescope. Eight solid state detectors, each 3 mm thick and 4.5 cm2 in area are used individually and in coincidence as total absorption spectrometers. Varying depths of tungsten absorber are between each Di element.

For more information, refer to the document:

D.E.Stillwell, W.D.Davis, R.M.Joyce, F.B.McDonald, J.H.Trainor, W.E.Althouse, A.C.Cummings, T.L.Garrard, E.C.Stone, and R.E.Vogt, "The Voyager Cosmic Ray Instrument", ISEE Transactions on Nuclear Science, Vol. 26, 1979, pp. 513

DATA_SET_PARAMETERS:

Time of start of averaging interval in seconds from start of base year, TIME;

6 hour averages of the following fluxes, plus statistical errors units of particles/(cm**2.sec.ster.MeV/nuc) HELIUMFLUXi or PROTONFLUXi ;

6 hour averages of the following rates, plus statistical errors units of particles/second

The following diagrams are given to assist the user in understanding the meaning of the data quantities present.

Simplistic diagram of Voyager instruments:

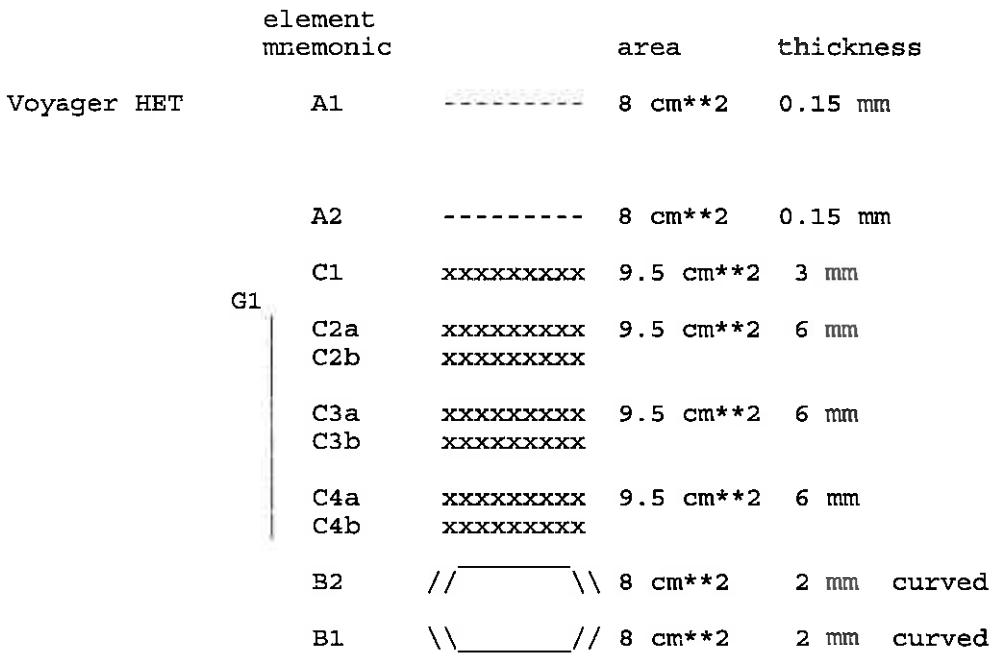

light baffle

L1 ---------- 2.8 cm**2 surface barrier 35 uM

L2 ---------- 2.8 cm**2 surface barrier 35 uM

L3 xxxxxxxxx 4.5 cm**2 surface barrier 450 uM

L4 xxxxxxxxx 4.5 cm**2 surface barrier 450 uM

Voyager TET

D1 xxxxxxxxx

D2 xxxxxxxxx
.25 mm tungsten absorber

D3 xxxxxxxxx
.56 mm tungsten absorber

D4 xxxxxxxxx
1.12 mm tungsten absorber

D5 xxxxxxxxx
1.60 mm tungsten absorber

D6 xxxxxxxxx
2.03 mm tungsten absorber

D7 xxxxxxxxx
2.34 mm tungsten absorber

D8 xxxxxxxxx

Di detectors= 4.5 cm**2 Lithium drifted 3mm
tungsten absorbers are 18.0 g/cm**3

where cm = centimeters
mm = millimeter
where uM = micrometer

Data present on our tape(s) :
Time in seconds from start of base year, for start of averaging interval

Particle fluxes are given in units particles/(cm**2.s.sr.Mev/n)
Rates are given in units particles/s
where cm = centimeters
s = second

sr = steradian

Underneath the flux designations, HELIUMFLUX1, for example, is a mnemonic code, such as M IIA2, indicating from which calibration response table this data came from. It is for documenting purposes only.

In the following, the phrases "2 dimensional analysis" or "3 dimensional analysis" refer to events whose analysis utilized pulse height data from either 2 or 3 pulse height values associated with the particular event type (detector element coincidence requirement) being measured at the time. As an example, for A side events, particles enter the HET telescope from the A end, and 1) stop in A1 or A2 for 2-dimensional A stopping events
2) stop in the C123 stack for 3-dimensional A stopping events
3) pass entirely through the SumC stack and have a B1 or B2 pulse height as well and are called 3-dimensional A penetrating events.

HET fluxes :

HELIUMFLUX1 M IIA2	Helium4 flux in particles/cm**2.s.sr.Mev/n A-stopping 2 dimensional analysis, high gain data from HET-II 4.2 - 6.0 MeV energy range
HELIUMFLUX2 M IIA3	Helium4 flux as above, A-stopping, 3 dimensional analysis, high gain data from HET-II 6.0 - 42.0 MeV energy range,
HELIUMFLUX3 M IIL2	B-stopping 2 dimensional analysis, low gain HET-II 17.0 - 27.0 MeV
HELIUMFLUX4 M IIL3	B-stopping 3 dimensional analysis, low gain HET-II 30.0 - 69.0 MeV
HELIUMFLUX5 M IIB2	B-stopping 2 dimensional analysis, high gain HET-II 17.0 - 27.0 MeV
HELIUMFLUX6 M IIB3	B-stopping 3 dimensional analysis, high gain data from HET-II 30.0 - 69.0 MeV
HELIUMFLUX7 M IIP	B-penetrating 3 dimensional analysis, low gain penetrating data from HET-II 193.125 - 480.486 MeV
HELIUMFLUX8 M IIPH	B-penetrating 3 dimensional analysis, high gain penetrating data from HET-II 191.925 - 475.705 energy range

```
---------------------------------
PROTONFLUX1              Proton  flux in particles/cm**2.s.sr.MeV/n
M IIA2                   A-stopping 2 dimensional analysis, high
                         gain data from HET-II
                         4.2 - 6.0 MeV energy range
---------------------------------
PROTONFLUX2              Proton  flux in particles/cm**2.s.sr.MeV/n
M IIA3                   3 dimensional analysis, high gain data from
                         HET-II
                         6.0 - 42.0 MeV energy range,
---------------------------------
PROTONFLUX3              B-stopping 2 dimensional analysis, high
M IIB2                   gain data from HET-II
                         17.0 - 27.0 energy range
---------------------------------
PROTONFLUX4              B-stopping 3 dimensional analysis, high
M IIB3                   gain data from HET-II
                         30.0 - 69.0 energy range
---------------------------------
PROTONFLUX5              B-penetrating 3 dimensional analysis, high
M IIPH                   gain penetrating data from HET-II
                         132.834 - 241.963 energy range
---------------------------------
LET fluxes :   (all stopping particle events)
---------------------------------
P PROTON
* M LC2                    NO LC2 RESPONSE FOR V1 is AVAILABLE
* B    1.800     3.300
---------------------------------
PROTONFLUX6               Proton 2-dimensional analysis from LET-D
M LD2                       energy range of 1.8 - 3.3 MeV
---------------------------------
PROTONFLUX7               Proton 3-dimensional analysis from LET-C
M LC3                       energy range of 3.25 - 8.1 MeV
---------------------------------
PROTONFLUX8               Proton 3-dimensional analysis from LET-D
M LD3                       energy range of 3.25 - 8.1 MeV
---------------------------------
P ALPHA
* M LC2                         NO LC2 RESPONSE FOR V1 is AVAILABLE
* B    1.800     2.800
---------------------------------
HELIUMFLUX9               Helium4 2-dimensional analysis from LET-D
M LD2                     1.800 - 2.800 MeV energy range
---------------------------------
HELIUMFLUX10              Helium4 3-dimensional analysis from LET-C
M LC3                     2.800 - 8.000 MeV energy range
---------------------------------
HELIUMFLUX11              Helium4 3-dimensional analysis from LET-D
M LD3                     2.800 - 8.000 MeV energy range
---------------------------------
---------------------------------
HET   event type RATES (for flux calculations) :
---------------------------------
*   NOMINAL COINCIDENCE CONDITION status
*   exists unless otherwise noted.
*   To interpret the LOGIC EQUATIONS (refer to simplistic telescope
*   diagrams above) :  EXAMPLE:  BRIBSP (the BR pre-mnemonic
*   indicates to our system a rate bin request and is left here for
```

```
*   documentation purposes only)
*              B1.B2.^SB.^C1.^G1.^A2
*   The above LOGIC EQUATION means: a particle entered the
*   telescope from the B end, and met the coincidence condition of
*   passing through B1, stopping in either B2 or the C432 stack,
*   but NOT (= ^ ) tripping the Slant threshold condition SB,
*   NOT going into C1, Guard G1, or A2.
*
---------------------------------
HET-I event type rates (for flux calculations) :
---------------------------------
BRIAS                          A-Stopping High Gain
  A1.A2.^C4.^G1.^B2

BRIASZ3                        A-Stopping Low Gain  Atomic Number
                                    Z >= 3
  A1.A2.SA.^C4.^G3.^B2

BRIBSE                         B-Stopping electron event
  B1.B2.C4.^SB.^C1.^G1.^A2

BRIBSP                         B-Stopping High Gain
  B1.B2.SB.^C1.^G1.^A2

BRIBSZ2                        B-Stopping Low Gain  Atomic Number
                                              Z >= 2
  B1.B2.SB.^C1.^G3.^A2

BRIPENH                        B-Penetrating High Gain
  B1.B2.C1

BRIPENL                        B-Penetrating Low Gain
  B1.B2.C1

BRIPGH                         Guard High Gain
  B1.B2.C1.^G1

BRIPGL                         Guard Low Gain
  B1.B2.C1.^G1

BRIBS4E
  B1.B2.C4.^C3.^SB.^G1         Stop in C4, did NOT get into C3

BRIBS4P
  B1.B2.C4.^C3.SB.^G1                "                          , High
                                                                  Gain

BRIBS4
  B1.B2.C4.^C3.^SB.^G1               "

BRIBS4Z2
  B1.B2.C4.^C3.SB.^G1                "                          , Low
                                                                  Gain

BRIBS3E
  B1.B2.C4.C3.^C2.^SB.^G1      Stop in C3, did NOT get into C2, High
                                                                  Gain

BRIBS3P
```

```
  B1.B2.C4.C3.^C2.SB.^G1          "

BRIBS3
  B1.B2.C4.C3.^C2.^SB.^G1         "

BRIBS3Z2
  B1.B2.C4.C3.^C2.SB.^G1          "                          , Low
                                                              Gain

BRIBS2E
  B1.B2.C4.C3.C2.^C1.^SB.^G1  Stop in C2, did NOT get into C1, High
                                                              Gain

BRIBS2P
  B1.B2.C4.C3.C2.^C1.SB.^G1       "

BRIBS2
  B1.B2.C4.C3.C2.^C1.^SB.^G1      "

BRIBS2Z2
  B1.B2.C4.C3.C2.^C1.SB.^G1       "                          , Low
                                                              Gain

-----------------------------------
HET-II event type RATES (for flux calculations) :
  interpreted analagously to HET-I
-----------------------------------
BRIIAS
  A1.A2.^C4.^G1.^B2

BRIIASZ3
  A1.A2.SA.^C4.^G3.^B2

BRIIBSE
  B1.B2.C4.^SB.^C1.^G1.^A2

BRIIBSP
  B1.B2.SB.^C1.^G1.^A2

BRIIBSZ2
  B1.B2.SB.^C1.^G3.^A2

BRIIPENH
  B1.B2.C1

BRIIPENL
  B1.B2.C1

BRIIPGH
  B1.B2.C1.^G1

BRIIPGL
  B1.B2.C1.^G1

BRIIBS4E
  B1.B2.C4.^C3.^SB.^G1

BRIIBS4P
  B1.B2.C4.^C3.SB.^G1
```

```
BRIIBS4
  B1.B2.C4.^C3.^SB.^G1

BRIIBS4Z2
  B1.B2.C4.^C3.SB.^G1

BRIIBS3E
  B1.B2.C4.C3.^C2.^SB.^G1

BRIIBS3P
  B1.B2.C4.C3.^C2.SB.^G1

BRIIBS3
  B1.B2.C4.C3.^C2.^SB.^G1

BRIIBS3Z2
  B1.B2.C4.C3.^C2.SB.^G1

BRIIBS2E
  B1.B2.C4.C3.C2.^C1.^SB.^G1

BRIIBS2P
  B1.B2.C4.C3.C2.^C1.SB.^G1

BRIIBS2
  B1.B2.C4.C3.C2.^C1.^SB.^G1

BRIIBS2Z2
  B1.B2.C4.C3.C2.^C1.SB.^G1

-----------------------------------
HET-I singles rates
-----------------------------------
BRIA1H                      Singles rate, high gain, for the A1
  A1                           element
                            below are all high gain until noted
BRIA2H
  A2

BRIC1H
  C1

BRIC2H
  C2

BRIB1H
  B1

BRISBH
  SB

BRIC3H
  C3

BRIC4H
  C4

BRIB2H
```

```
  B2

BRIG1
  G1

BRIA1L                    begin low gain singles here
  A1

BRIA2L
  A2

BRIC1L
  C1

BRIC2L
  C2

BRIB1L
  B1

BRISA1
  SA

BRISA2
  SA

BRISBL
  SB

BRIC3L
  C3

BRIC4L
  C4



BRIB2L
  B2

-----------------------------------
HET-II singles rates
  Interpreted the same as HET-I singles rates
-----------------------------------
BRIIA1H
  A1

BRIIA2H
  A2

BRIIC1H
  C1

BRIIC2H
  C2

BRIIB1H
  B1
```

```
BRIISBH
  SB

BRIIC3H
  C3

BRIIC4H
  C4

BRIIB2H
  B2

BRIIG1
  G1

BRIIA1L                        begin low gain singles here
  A1

BRIIA2L
  A2
BRIIC1L
  C1

BRIIC2L
  C2

BRIIB1L
  B1



BRIISA1
  SA

BRIISA2
  SA

BRIISBL
  SB

BRIIC3L
  C3

BRIIC4L
  C4

BRIIB2L
  B2

-----------------------------------
LET singles rates  in high gain
-----------------------------------
BRLA1
  L1

BRLA2
  L2
```

BRLA3
L3

BRLA4
L4

BRSLA
SL

BRSLB
SL

BRLB1
L1

BRLB2
L2

BRLB3
L3

BRLB4
L4

BRLC1
L1

BRLC2
L2

BRLC3
L3

BRLC4
L4

BRSLD
SL

BRLD1
L1

BRLD2
L2

BRLD3
L3

BRLD4
L4

TET singles rates H or L at end of rate indicates High or Low Gain

---

BRD6L
D6

```
BRGA+GB
  GA.GB

BRD5H
  D5

BRD7L
  D7

BRD6H
  D6
BRD7H
  D7

BRD5L
  D5

BRD8L
  D8

BRD1H
  D1

BRD4H
  D4

BRD2L
  D2

BRD3L
  D3

BRD1L
  D1

BRD3H
  D3

BRD2H
  D2

BRD4L
  D4

*  MAJOR STATUS CHANGE CONFIGURATIONS IN CRUISE AFFECT THESE
-----------------------------------
LET event type rates (for flux calculations) :
-----------------------------------
BRLATRP
  L1.L2.^L4

BRLBTRP
  L1.L2.^L4

BRLCTRP
  L1.L2.L3.^L4

BRLCTRP
  L1.L2.^L4
```

```
BRLDTRP
  L1.L2.^L4

BRLC                        High Gain  (typical mnemonic)
  L1.L2.L3.^SL.^L4
BRLC
  L1.L2.^SL.^L4

BRLCZ3                      Low Gain  Atomic Number Z >= 3
  L1.L2.L3.SL.^L4                (typical mnemonic)

BRLCZ3
  L1.L2.SL.^L4

* LD                          NOMINAL DEFINITION IS PRESENT
*                     near launch FOR LA, LB, LD SERIES
* L1.L2.L3.^SL.^L4
BRLD
  L1.L2.^SL.^L4

* LDZ3                        NOMINAL DEFINITION IS PRESENT
*                     near launch FOR LA, LB, LD SERIES
* L1.L2.L3.SL.^L4

BRLDZ3
  L1.L2.SL.^L4

BRLA
  L1.L2.^SL.^L4

BRLAZ3
  L1.L2.SL.^L4

BRLB
  L1.L2.^SL.^L4

BRLBZ3
  L1.L2.SL.^L4

-----------------------------------
TET event type rates (for flux calculations) :
-----------------------------------
BRTAN
  W1.W2.D3.^D8.^GA.^GB

BRTAN
  W1.W2.^D8.^GA.^GB

BRTLO
  W1.W2.D3.D5.^D6.^GA.^GB.^UT

BRTLO
  W1.W2.D5.^D6.^GA.^GB.^UT

BRTHI
  W1.W2.D3.D7.^D8.^GA.^GB.^UT

BRTHI
```

W1.W2.D7.^D8.^GA.^GB.^UT

Description of DATA

Files of data are in ASCII text format, variable length formatted records, readable by the example program given below. The records of these datasets contain words with information on start time, data quantities are present, the averaging interval , and ASCII character data descriptions of the specific coincidence logic condition which gives rise to the data quantity being presented.

If the Error value is -1.0, data for this item is not available. If the Flux and Error are 0.0 no events occurred during the collection time.

The format of the text data is generally as follows:

Record #:	general length	description
1	C*12	Satellite name
2	C*n	Start time of first 6 hour average present
3	C*n	Stop time of last 6 hour average present
4	C*3	Number of bins (data quantities present)

Records 5-(N+4) (where N = number of bins): Bin Label Records

C*3	bin number
C*n	Character data label description

Records N+4- ... Data records:

C*19	Start time as yy-mm-ddThh:mm:ss
C*15	Value of data quantity 1
c*15	Error in data quantity 1
.	.
.	.
C*15	Value of data quantity N
C*15	Error in data quantity N

This program will list the contents of the data for one quantity.

```
C       EXTRACTS SPECIFIED ITEM FROM A VOYAGER NSSDC FORMATTED FILE
        IMPLICIT NONE
        CHARACTER*12 SATID
        CHARACTER*19 START,END,T
        CHARACTER*132 LABEL
        CHARACTER*100 FMTSTRING
        CHARACTER*40 FNAME
        INTEGER I,IBIN,NOBINS
        REAL FLUX,ERROR
```

```
      WRITE (6,*) 'FILE:'
      READ(5,'((A))') FNAME
      OPEN(UNIT=1,FILE=FNAME,STATUS='OLD')
      READ(1,'((A))') SATID
      WRITE(6,'((A))') SATID
      READ(1,'((A))') START
      WRITE(6,'((A))') START
      READ(1,'((A))') END
      WRITE(6,'((A))') END
      READ(1,*) NOBINS
      WRITE(6,*) 'BIN NUMBER:'
      READ(5,*) IBIN
      IF ((IBIN .LT. 1) .OR. (IBIN .GT. NOBINS)) THEN
           WRITE(6,*) 'BIN # ',IBIN,' NOT IN RANGE (1,',NOBINS,').'
                STOP
      ENDIF
      WRITE(FMTSTRING,1) 2*(IBIN-1)*15
1     FORMAT('((A),',I5,'X,2E15.5)')
      DO 10 I=1,IBIN-1
         READ(1,'((A))') LABEL
10    CONTINUE

      READ(1,'((A))') LABEL
      WRITE(6,*) LABEL

      DO 20 I=IBIN+1,NOBINS
         READ(1,'((A))') LABEL
20    CONTINUE

      DO 30 I=1,1000000
         READ(1,FMTSTRING,END=100) T,FLUX,ERROR
         WRITE(6,25) T,FLUX,ERROR
25       FORMAT(1X,A19,1X,2E15.5)
30    CONTINUE
      STOP
100   WRITE(6,*) 'END OF FILE'
      STOP
      END
```

DATA_SET_QUALITY/INSTRUMENT_PERFORMANCE:

Three status configurations have been used in the CRUISE portions of the mission (see below).

The LET and TET are in non-nominal status states for much of the CRUISE portion of the mission. To access non-nominal rate data in our system requires input to our FLUXPLOT program (which makes data summaries) of the exact COINCIDENCE LOGIC EQUATION described by the non-nominal instrument status. To handle both nominal and non-nominal times we have requested both states for the lifetime cruise periods. Therefore, users of this NSSDC data need to be aware of the correct status condition for times of interest, and look at the corresponding data quantity for our submission, in order not to be

confused by thinking there is no data for those quantities affected.

The exact order of data on our tapes is listed after the REFERENCES section of this header information.

VOYAGER-1 CRUISE PERIODS (NON-ENCOUNTER) STATUS SUMMARIES

```
VOLUME time
------ ----
24832  9/16/77 15:45: 0    IN STATUS CONFIG (1)
 STATUS CONFIG (1) = NOMINAL + 0020 0580 0680 0780 0880       0D0A
60948  9/27/78 20:45:0     IN STATUS CONFIG (2)
 STATUS CONFIG (2) = NOMINAL + 0020 0580 0600 0780 0880 0A04 0D0A
287502 3/14/85 19:15:0     IN STATUS CONFIG (3)
 STATUS CONFIG (3) = NOMINAL + 0020 0580 0600 0780 0880 0A00 0D0A
```

Telescope nominal conditions are indicated by a 00 in the right-most byte of each status word for words 5 - 10 (05 - 0A in the left byte of each status word).

status byte meanings:

0020	High Volt. enable indicator
0580	delete LA3 terms
0600	nominal
0680	delete LC3 terms
0780	delete LB3 terms
0880	delete LD3 terms
0A00	nominal
0A04	delete D3 terms
0D0A	Het 1 and Het 2 auto gain flag on

other status byte values sometimes used:

0D05	Het 1 and Het 2 gain set high

excluded data times (localized and non-localized data blips):
These times have been excluded from our NSSDC data:

```
SE         77/09/18 00:00:00 77/10/03 00:00:00
SE         77/10/12 00:00:00 77/10/15 00:00:00
SE         77/11/10 00:00:00 77/12/01 20:00:00
SE         78/04/08 00:00:00 78/06/07 00:00:00
SE  *      78/05/23 05:30:00 78/05/23 06:00:00
SE         78/06/23 00:00:00 78/06/29 00:00:00
SE  *      78/07/01 03:30:00 78/07/01 04:00:00
SE         78/07/02 00:00:00 78/07/06 00:00:00
SE         78/07/08 00:00:00 78/07/21 00:00:00
SE  *      78/09/27 13:30:00 78/09/27 20:45:00
SE  *      78/11/21 18:45:00 78/11/21 19:00:00
SE  *      78/12/18 08:45:00 78/12/18 09:00:00
SE  *      78/12/28 08:15:00 78/12/28 08:30:00
SE  JUP    79/02/15 00:00:00 79/03/22 00:00:00
SE  *      79/03/19 00:00:00 79/03/21 23:15:00
SE  *      79/08/15 02:15:00 79/08/15 03:00:00
SE         80/03/14 00:00:00 80/03/15 00:00:00
SE  *      80/10/25 15:45:00 80/10/26 02:15:00
SE  SAT    80/11/12 00:00:00 80/11/23 00:00:00
SE         81/10/13 00:00:00 81/11/14 00:00:00
```

```
SE  *     81/10/30 18:00:00 81/10/31 01:30:00
SE  *     81/11/06 04:00:00 81/11/06 04:30:00
SE        83/08/15 00:00:00 83/08/16 00:00:00
SE        83/08/23 00:00:00 83/08/24 00:00:00
SE        86/12/05 08:00:00 86/12/05 12:00:00
SE        87/03/04 07:00:00 87/03/04 10:00:00
SE        87/03/16 05:00:00 87/03/16 10:00:00
SE        87/07/21 00:00:00 87/07/22 00:00:00
SE        87/07/22 07:00:00 87/07/22 10:00:00
SE        87/10/11 06:00:00 87/10/11 07:00:00
SE  *     88/02/06 20:30:00 88/02/06 23:45:00
SE        88/05/26 09:00:00 88/05/26 10:00:00
SE  *     88/11/02 05:00:00 88/22/02 05:15:00
SE  *     89/12/12 17:15:00 89/12/12 17:45:00
```

Whole single exclude days are probably data blips which were never localized.

* indicates time derived from status listings

Voyater-1 Encounter times:

```
   Jupiter   5Mar79  for exclude use 2/15/79 - 3/22/79
                          VOLUMEs    74401   - 77758
   Saturn   12Nov80                 11/02/80 - 11/23/80
                          VOLUMEs   134497   - 136513
```

Year timeline summary
Instrument condition /general health observations:

2/8/82 PHA BLOCK for LETA,B, HET I partial failure

TAN event type rates need special coincidence equations during part of cruise: for TAN, TLO, THI
delete the D3 term from
9/27/78 20:45 - 3/14/85 19:15

LET event type rates need special coincidence equations during cruise: for LA,LB,LD high and low gains
delete the L3 term throughout the mission
For LC set, delete L3 from launch - 9/27/78 20:45;
then LC set is nominal

1977 Status Configuration 0 essentially nominal at launch
Status Configuration 1 begins at 9/16/77 15:45

1978 day 100 - 160 bad times; (day 190-200 bad data/gap He ASTP)
Status Configuration 2 begins at 9/27/78 20:45

1979 day 45 - 80 Jupiter; (day 100 - 112 bad data? He IA2,IIA2)

1980 day 316 - 323 Saturn

1981

1982 2/8/82 PHA BLOCK for LETA,B, HET I partial failure

-et IPH, IP; IB3 electron ; all gone
-et LA2,3 LB2,3 H data there, but la2, lb2 drop 10+1
other H data have calib discrepancy from then on;
He is present everywhere, but with sparse periods and
no notes on calibration discrepancy
-HET I,II calibration discrepancy IA2,IA3 H, HE from then on,
and sparseness in data after day 300 of 1985; flux
discrepancy disappears after day 140 of 1989 (a)

1983

1984

1985 day 300 -> (a)

Status Configuration 3 begins at 3/14/85 19:15

1986 ----------(a)----------

1987 ----------(a)----------

1988 ----------(a)----------

1989 ---(a)-------~day 140.

1990

1991

1992

(a) After day 40 of 1982, our group uses only HET II for fluxes
The gap of day 315-335, 1977 where indicated was caused by an
exclude card, added to prevent FLUXPLOT from
returning invalid fluxes related to a data exception
it did not handle properly.

HE IB2,IIB2 all ok, but H IB2,IIB2 has flux discrepancy after ~day
160 of 1982

Dr. A. Cummings (Principle Investigator, CIT) has provided the
following information from the theses indicated, to summarize
instrument health and experiment problems.

START OF THESIS INFORMATION ----------
From the Rick Cook thesis-

Appendix B Problems

B.1 LET B of Voyager-1

The response of this telescope was unusual in that (1) the HE

mass measurement, M1, showed a relatively large energy and time dependence, (2) a relatively large 'background' of events was present in the charge range near fluorine, and (3) the L1 versus L2+L3 element tracks had an uncharacteristically blurred appearance. The problem may be electronic instability, but was not investigated in detail; instead the data from this telescope were excluded from use in the measurements presented in Chapter 4, Tables 4.1 through 4.12.

B.2 LET C of Voyager-2

On April 1, 1978 the L1 detector of this telescope experienced a simultaneous shift in energy calibration and increase in count rate, perhaps as the result of a light leak in the thin AL entrance window. Subsequent data from this telescope were not used in the measurements of Chapter 4, Tables 4.1 through 4.12.

B.3 Pulse Height Multiplication in the LET 35 um Detectors

A background effect specific to the iron group nuclei was identified in Sections 3.3 and 3.5 and necessitated the further study and special handling which is discussed here. The affected PHA events were clearly seen in Figure 3.7, a plot of the charge measurements Z1 versus Z2, as a clump of points near (Z1=26, Z2=28). Inspection of the L1, L2 and L3 pulse heights of the events in this clump revealed a very specific signature:

(1) The events lie directly on the L1 versus L3 track for iron, but lie just above the L2 versus L3 iron track, indicating that the L1 and L3 pulse heights are normal, but that the L2 pulse height is abnormally large.

(2) The events have relatively small L3 pulse heights (E{L3} less than about 170 MeV), indicating that the nuclei responsible for the events just barely penetrated detector L2.

The effect also occurs for a fraction of the iron nuclei which barely penetrate the L1 detectors. In this case, the affected events may be seen as the unusual clump of points near Z1=28 in Figure 3.6.

The above signature suggests a pulse height multiplication effect in the LET 35 um surface barrier detectors that is very similar to one observed earlier in the response of such detectors to fission fragments. The effect (discussed by Walter 1969) occurs for nuclei which deposit a large ionization charge density in the depleted silicon near the gold electrode. The large ionization charge density is thought to induce tunneling of additional carriers (electrons) from the electrode through the thin oxide layer which separates the electrode frm the depleted bulk silicon. The orientation of the LET 35 um detectors is consistent with this multiplication hypothesis: The gold electrodes face toward the L3 detector, such that the ionization charge density near a gold electrode is largest for nuclei which just barely penetrate the detector, as in (2) above.

To further stydy the problem, three detector PHA events with charge measurements Z1> 24 were re-analyzed. For each event the L1 and L3 energy measurements (E{L1} and E{L3}) were used to calculate a new charge measurement Z' and obtain an estimate E'{L2} of the energy deposited in detector L2 by solving:

$$T\{L1\} = R(E\{L1\} + E'\{L2\} + E\{L3\},\ Z',\ M) - R(E'\{L2\} + E\{L3\},\ Z',\ M)$$

$$T\{L2\} = R(E'\{L2\} + E\{L3\},\ Z',\ M) - R(E\{L3\},\ Z',\ M)$$

taking $M = 2.132 * Z'$

R is the generalized range-energy function discussed in Section 3.4. T{L1} and T{L2} are the mean pathlengths for the L1 and L2 detectors respectively. The results are illustrated in Figure B.1, a plot of E{L2} (the measured L2 energy) versus E'{L2} (the L2 energy inferred from the L1 and L3 energy measurements). Normal events lie along the diagonal, while events with abnormally large L2 energy measurements lie above the diagonal. (Events below the diagonal may be due to L2 edge effects and other processes discussed in Section 3.5.2) The abnormal events occur predominantly at large values of E'{L2} which can only be obtained by nuclei which barely penetrate L2, consistent with observation (2) above. Figure B.2 shows two histograms of E{L2}/E'{L2} ; one histogram for events which barely penetrate L2 (E{L3} < 170 MeV) and one for the remaining events (E{L3} > 170 MeV). These histograms are summed over all the LETs used on both Voyagers and indicate that (1) about 15 percent of the events with E{L3} less than 170 MeV have L2 energy measurements which are abnormally large by an average of about 12 percent and (2) the L2 energy measurements are essentially normal for events with E{L3} greater than 170 MeV.

B.3.1 Three Parameter Analysis for Iron Nuclei

The results for iron nuclei presented in Table 4.2 (8.7-15.0 MeV/nucleon) are based on PHA events selected as follows:

(1) Normal iron events (i.e. those with normal L2 pulse height) were selected using the charge consistency requirement and charge boundaries discussed in Section 3.5, and were counted if the total energy measurement, E{L1}+E{L2}+E{L3}, was appropriate to the 8.7 - 15.0 MeV/nucleon interval.

(2) Iron PHA events having abnormally large L2 pulse heights were identified as those events with charge measurements near (Z1=26, Z2=28). (Specifically, the requirement was (Z1+Z2)/2 > 25 and (Z1-Z2) < -0.85.) For each of the PHA events the L2 energy measurement was divided by 1.125 (the mean shift of the abnormal L2 energy measurements; see Figure B.2) to obtain a corrected value E*{L2}. Then the event was counted if E{L1}+E*{L2}+E{L3} was within the total energy interval corresponding to 8.7 - 15.0 MeV/nucleon.

PHA events with abnormal L2 pulse heights constitute about 15 percent of the iron nuclei counts presented in Table 4.2. Any additional systematic error (beyond that discussed in Section 4.4.1) in the iron nuclei counts due to the abnormal L2 pulse heights should be small. For example, if no corrections at all are applied to the abnormal L2 energy measurements (as was the case for the iron abundances reported earlier in Cook et. al. 1979 and Cook, Stone and Vogt 1980), the resulting iron abundance measurements differ from those of Table 4.2 by less than 5 percent.

B.3.2 Two Parameter Analysis for Iron Nuclei

In the two parameter analysis of iron (for the fluence measurements of Tables 4.4 through 4.11) the multiplication effect in the L1 detectors was taken into account as follows:

(1) Iron PHA events with normal L1 pulse heights were identified as those events with charge measurement Z1 in the range 24.8 to 27.2 and were binned according to energy/nucleon as described in Section 3.4.

(2) PHA events with charge Z1 in the range 27.2 to 32.0 and L2+L3 energy measurements of less than 170 MeV are primarily due to iron nuclei with abnormally large L1 pulse heights, rather than nickel or other nuclei. Therefore, the L1 energy measurements of these events were divided by 1.125 before energy/nucleon binning. The remaining events with Z1 in the range 27.2 to 32.0 (i.e. those with E{L2}+E{L3} > 170 MeV) are mainly nickel nuclei an were included with no L1 energy adjustment. All PHA events were sorted into energy/nucleon binns as if they were due to iron nuclei, exactly as in (1) above.

In the two parameter iron analysis, no special treatment was applied to account for multiplication effects in the L2 detectors. They do not significantly affect the Z1 charge measurement and at most shift a small fraction (about 5 percent) of the PHA events which should fall in th 7.8-8.7 MeV/nucleon interval into the 8.7 - 10.6 MeV/nucleon interval.

The inclusion of nickel and other nuclei (27 <= Z <= 32) increases the fluence measurements over measurements of pure iron by roughly the combined abundance of these elements relative to iron, or about 10 percent. However, the inclusion of these nuclei probably has only a negligible effect on the spectral index(gamma, see Section 4.5), since the energy spectra of the various elements of the iron group are likely to be similar. (Spectral index variations among the elements appear to be roughly ordered by nuclear charge Z, such that, in a given flare event, neighboring elements have similar spectral indices; see Section 5.2. Further, the nickel to iron ratio {8.7 -15 MeV/nucleon, Table 4.2} is nearly constant from flare to flare.)

The multiplication effect in the L1 detectors is potentially an additional source of systematic error (beyond those discussed in Section 4.5) in the iron fluence measurements of Tables 4.4 through 4.11 and the iron spectral index measurements of Tabl 4.12. Upper limits to these possible additional errors were obtained by re-computing the fluences and spectral indices without the L1 energy corrections discussed in (2) above. The changes in the iron fluence measurements were typically less than 10 percent for energy bins in the range 5.0-8.7 MeV/nucleon, and wer zero for the other higher energy bins. The iron spectral indices changed by less than 5 percent. Since the actual systematic error induced in the iron spectral indices is probably much less than 5 percent (and therefore is small compared to statistical error and the possible systematic error from other sources discussed in Section 4.5) this error is negligible.

HH Breneman Thesis. Flare analysis treated differently from

interplanetary data.

Appendix G Instrumental Anomalies and Other Problems

The analysis of data form the Voyager CRS LET and HET telescopes was complicated by several instrumental problems. These are described in detail elsewhere (Breneman 1984); they are summarized here.

G.1. Pulse Height 'Multiplicaton' Effect

This effect has been observed many times in numerous surface-barrier detectors, both in flight and in the laboratory (Cook 1981, Breneman 1982). Particles passing completely through a detector sometimes yield pulse heights that are anomalously high By about 10 - 30 %). It occurs most often for particles with high dI/dx in the detector in question, and therefore at a given initial energy, the errect occurs more often for elements higher on the charge scale; in the data it is most prominent for Fe. On a delta E versus E' plot, the effect appears as a more or less diffuse 'track' above and roughly parallel to the nominal track for the element, since delta E is anomalously high for the affected particles (Fig. G.1). A charge determination of such an event will of course be high, generally by ~2-3 charge units at Fe. Since the effect is strongly dependent on dE/dx, it is usually evident only in the delta E detector immediately before the E' detector. When z is calculated for 3-parameter events involving such anomalous pulse heights, Z2 is more strongly affected than Z1, since the anomalous pulse height has the role of delta E for Z2, while for Z1 the same detector PHA usually makes only a modest contribution to E' with delta E normal. On a Z1 versus Z2 plot (e.e., Fig. 3.1), the effect takes the form of a cluster fo events to the right of, and slightly above, the main cluster along the diagonal. All of the Voyager LETs show the effect for Fe; although its rate of occurrence varies somewhat between the different telescopes, it is generally in the range of ~5 - 10 % of all the 3-parameter Fe SEP events in a given telescope. The fraction of 2-parameter events affected is larger, since the E' detector is thinner and therefore a larger fraction of the data has high dE/dx in the delta E detector. At least one LET (Voyager 1 LET A) shows evidence for the effect at charges as low as 20.

In the HETs the problem is worse in several respects. Its rate of occurrence at Fe, as a percentage of the total Fe event ample, is generally much larger than in the LETs (~40 % for Voayger 1 HET 2); it is clearly seen for elements as low on the charge scale as Mg in some telescopes (Voyager 1 HET 2 and Voyager 2 HET 2); and for 3-parameter events it can sometimes be seen occurring in either (or both) delta E detectors, rather than just the last one, resulting in several displaced clusters of events in those telescopes (Voyager 1 HET 1 and Voayger 2 HET 2).

Two actions were necessary to deal with this problem. For abundant elements affected by the problem, mainly Fe and Ni, the 3-parameter charge consistency requirement was made lenient enough to include the particles affected by pulse

height multiplication. The rate of occurrence in LET for elements lower than Fe was negligible compared to other sources of uncertainty in the abundance determination, and no correction was made for these elements. Based on the observed rates in some HET telescopes for the abundant elements (e.e., Fig. G.2 for Voayger 1 HET 2), the rate of occurrence in these thelscopes for elements in the Z = 17-25 charge range was significant even though limited statistics make it less apparent and less quantifiable. However, HET data were not used for these elements for the reasons given in Section 3.3.

In addition, the energy loss in the delta E detector had to be corrected in an approximate way for affected events, so that the total incident energy, which is required for constructing energy spectra, would be accurate.

For 2-parameter events, there is no second independent determination fo Z to permit unambiguous separation of normal and abnormal events. This is not a serious problem for abundant elements, since the only abundant element significantly affected is Fe, which has no other elements of comparable abundance near it on the charge scale with which it could be confused. For rare elements the situation would be more serious, but as noted in Section 3.3, 2-parameter data were not used for rare element abundances due to excessive background contamination from other sources.

G.2. LET Telescope ID Tag Bit Errors at High Counting Rates

For each Block I or Block II LET event, there is a single tag bit which specifies from whih LET telescope in that Block the event originated. A near coincidence in the triggering of LETs A and B, as is possible during periods of very high count rates, can result in the bit being set for a LET A event, causing that event to be read out as a LET B event (similarly for C and D). Since the bit is ordinarily set only for LET B events and is otherwise not set, LET A events can be misidentified as LET B events but never the reverse.

The telescope identification bit is used in all subsequent data analysis to determine the appropriate detector thicknessess and gains to use in calculating energy losses in the detectors and, ultimately, the charge of the particle. If the telescope identification is erroneous, incorrect thick= nesses and gains are used in the calculations, resulting in incorrect determinations of Z. The magnitude and sign of the discrepancy in Z depends only on the (coincidental) relationship between the thicknesses of the detectors in the paired telescopes, and, to a lesser degree, differences in the energy calibrations fo the respective detectors.

On a Z1 versus Z2 plot of 3-parameter Voyager data, this effect has the appearance of small clusters of events displaced slightly from the main clusters along the diagonal for all the more abundant elements. It appears only in plots of the B and D telescopes, sine it is events with these identifications which contain some misidentified particles. In the Voyager flight data the effect is notice-

able only during flare period 7, for which the peak LET B singles rate is ~ 5 * 10**3 /sec, the highest seen during the Voayger mission through August 1984. Its rate of occurrence is about 3 % at this peak rate, an average of about 1 % for flare period 7 as a whole, and is the same for all elements for which statistics permit a measurement. On delta E versus E' plots of both 2- and 3-parameter data, these effects have the appearance of 'ghost' tracks falling between or partially overlapping the real tracks of nearby elements (Fig. G.3).

Later laboratory work using the backup GRS and pulse generators (Martin 1983) was able to reproduce the effect with greatly improved statistics, and verified the magnitude of the time constant (~6 us) implied by the flight data while extending coverage to event rates more than an order of magnitude above the highest seen in the flight data.

The impact of this problm on the data analysis is relatively minor. For 3-parameter data, the previously chosen charge-consistency requirement is restrictive enough to easily exclude the misidentified events; the amount of data lost is an insignificant 0.2% of the total, and the remaining data set is as 'clean' as that from the other telescopes. The problem is more serious for the 2-parameter data, since there is no second determination of Z to permit separation of the normal and abnormal events; it is an unremovable source of background in the data. For abundant elements this is unimportant, since the error introduced by this background is on the order of 1 % or less. But the problem would be serious for rare elements in cases where the 'ghost' trakc of an abundant element overlaps the true location fo a rare element, since even 1 % of an abundant element could seriously contaminate a much rarer element. However, as noted previously, the 2-parameter LET data are not useful in obtaining rare element abundances on account of other background contributions.

G.3. LET L1 Detector Jupiter Encounter Radiation Damage and Post-Encounter Annealing

As a result of their exposure to intense charged particle fluxes in the inner Jovian magnetosphere during the 1979 Jupiter encounters, the L1 detectors of the LETs experienced radiation damage which can be modeled as a reduction in the 'effective thickness' of the detectors. It is thought to be due to the implantation of energetic oxygen and sulfur ions known to be present in the inner Jovain magnetosphere (Gehrels 1982). Although all LETs on both spacecraft were affected to some degree, the Voayger 1 LETs were affected much worse than those on Voyager 2, since the former spacecraft passed closer to Jupiter and experienced a more intense radiation environment. On each spacecraft, LET C was by far the most seriously affected; this telescope was sparially oriented so as to receive the most intense radiation exposure during the Jupiter encounters. (LET B on Voyager 2 experienced unrelated types of radiation damage during the Jovian encounter and has returned no data since tha encounter.) The front detectors of the HETs, being much thicker than those of the LETs and pro-

tected by a thiker window, showed no detectable effective thichness reduction.

The impact of the radiation damage on the post-Jupiter data is apparent as a shift in the location fo the element tracks on a delta E versus E' plot of data from flares 16 and 17, the first large post-Jupiter flares, relative to their location in plots of pre-Jupiter flares. Similarly, Z1 versus Z2 plots of flares 16 and 17 show Z values shifted from their proper values when Z is calculated using the detector thicknesses measured before launch, which served adequately for all pre-Jupiter flares. The change in effective thickness appears to be somewhat dependent on Z, with the magnitude of the reduction increasing with Z for any given detector. Furthermore, with the passage of time the radiation damage seems to gradually undergo a partial reversal. This 'annealing' effect is evident in data from the later large flares, 20 and 24, which show less shift in Z than do the flares immediately following Jupiter encounter.

In the analysis of post-Jupiter data, this problem was dealt with by adjusting the L1 detector thicknesses used in the calculation of Z so as to make the calculated charges fall in the proper places on the charge scale. Flares 16 and 17 were used to define the required shift for the more abundant elements; a linear or weakly quadratic function of Z was fit to these to define the Z dependence for all Z. Data from flare periods 20 and 24 were used in conjunction with the flare 16/17 data to mathematically characterize the time-dependence of the annealing effect, by fitting to a decaying-exponential function of time. This procedure, repeated for each LET, defined the L1 thickness to be used in analyzing any given post-Jupiter event. The adjustment of the L1 thickness was then incorporated into the iterative cycle for calculating Z. The radiation damage did not have a noiceable effect on the inherent charge resolution of the telescopes, so with the above modifications the post-Jupiter flare data could be treated the same way as the pre-Jupiter data.

Table G.1 lists the adjustment made to the thickness for each L1 detector cor carbon and iron at two different times during the post-Jupiter phase. The actual expression for the thickness L(Z,t) of each L1 detector was given by

$$L(Z,t) = L0 - \text{deltaL0}(Z) + K \exp(\text{delta } t / 562.56)$$

where K is a constant, L0 is the pre-Jupiter thickness, delta t is the time since the Jupiter encounter in days, and deltaL0(z) is the linear or quadratic function of Z that closely fits the required thickness changes for the first post-Jupiter flares.

G.4. Voyager 2 LET C Temporary Gain Shift

During the time period 1978 APR 3 - June 9, the L1 detector of LET C on Voayger 2 experienced, for unknown reasons, a temporary gain shift (~ 47 % decrease) and an associated excessively high L1 count rate (~ 9* 10**3 /sec). The gain shift and excessive count rate set in abruptly, remained

nearly constant until about May 29, and then gradually reverted to their former levels; a very slight decline during the central phase was consistent with the decrease in the intensity of sunlight during the smae time period and suggests the possibility of a light leak in the telescope's aluminum window.

The effect on the data was to shift the locations of the element tracks on a delta E versus E' plot, and yield shifted charge estimates when nominal gain factors were used in the analysis. The only flares occurring duting this time period were the three large events of flare period 7. Since the gain was constant at the shifted value during these flares, the data could be analyzed by generating the appropriate gain factors by fitting the oxygen flight data from flare period 7 in the manner described in Appendix A. The resulting values are included in Table A.1.

This anomaly was previously noted (Cook 1981), and the telescope was rejected for analysis because of the problem. However, since the energy calibration used in the analysis is easily adjusted to compensate for the problem, since the charge resolution and background of the telescope do not seem to be affected by the problem and since the three 7 flares include a major fraction of all SEP data, it was decided to inlude Voayger 2 LET C in the analysis with the special treatment described above.

G.5 CRS Instrument Configuration Changes

At certain times during the Voayger mission, the configuation of the CRS instruments was changed in ways that influence data analysis. At the beginning of each flight the LETs were configured to require triggering of the L3 detector for pulse height analysis; that is, only 3-parameter events were analyzed. About 12 days after launch the L3 coincidence requirement was removed, permitting both 2- and 3-parameter events to be analyzed. For Voyager 2 this occurred before the first flares were seen, but on Voyager 1 flares 1a and 1b occurred before the configuration was changed, so no 2-parameter events were obtained from these flares. A similar situation occurred on 17 Jun 1978 when Voyager 1 LET C was switched back to requiring L3 coincidence. Thus for all flares from 8 onward there are no 2-parameter events from this telescope. These situations required changes in the weightings of 2-parameter relative to 3-parameter events for the affected spacecraft and flares. There could still be a residual abundance bias in flares 1a dna 1b if the particle composition was energy-dependent and if the two spacecraft saw particles with different spectra, but the possibility of a bias comparable to the statistical uncertainty in the abundances is very unlikely.

Another important configuration change is the HET gain state. Normally the instrument cycles between high and low gain modes, but after Jupiter encounter HET 1 on Voyager 2 was switched to a high-gain-only mode, so no post-Jupiter SEP heavy ion data were obtained from this telescope. This

required changes in the partile wwighting factors of HET relative to LET for Voyager 2 for all post-Jupiter flares.

The event weighting factors tabulated in Table 3.8 include the effects of all instrument configuration changes.

G.6. Voyager 1 Block I PHA Problem

On 1982 Feb 8, the Voayger 1 CRS experienced a failure affecting the readout of PHA information from the Block I telescopes (LETs A and B and HET 1). The result of the failure is that in place of PHA2, the instrument reads out whichever of the three PHAs has the largest numerical value. If PHA2 happens to be numerically the largest pulse height, as is true over some energy ranges, the event is read out normally; otherwise some information si lost. The effect of this problem is that some of the 2-parameter events are lost completely, and that some of the 3-parameter events are degraded to 2-parameter events.

The effect of this problem on the data analysis was minimal because it occurred very late in the time span included in the SEP data set, and thus affected only two relatively small flares. The problem was dealt with by simply discarding the data on these flares from the three telescopes affected.

END OF THESIS INFORMATION ----------

Summary of Voyager-1 LET L1 thickness and delta Z correction from Dr. Cummings:

LET L1 Thickness before VOLUME 94465

= 37.91 um LET A
30.91 um LET B
37.07 um LET C
35.45 um LET D
um = micrometers

LET L1 Thickness after VOLUME 94465

= 37.09 um + 0.82 {1 - exp{-(boi-94465)/943693} } LET A
27.97 um + 0.94 {1 - exp{-(boi-94465)/943693} } LET B
30.81 um + 6.26 {1 - exp{-(boi-94465)/943693} } LET C
34.68 um + 0.77 {1 - exp{-(boi-94465)/943693} } LET D
um = micrometers

Z1 is computed from L1 vs L2+L3 energies
After VOLUME 94465 Z1 is corrected as follows if Z1 > 9,
rho{123} = (E{L1}+E{L2}+E{L3}) / 2Z1 < 25

Z1' = Z1 + delta Z where

delta Z{A} = (Z1/26)**2 x (1.0461- 0.0418(rho{123})) x
{1 - exp{-(boi-94465)/943693} }

delta Z{B} = (Z1/26)**2 x (0.9254- 0.0370(rho{123})) x
{1 - exp{-(boi-94465)/943693} }

volumes in the library at the NCCS IBM 9021.

This data set is not intended to be used as an encounter data set.

LIT_REFERENCES:

INSTRUMENTATION

D.E.Stillwell, W.D.Davis, R.M.Joyce, F.B.McDonald, J.H.Trainor, W.E.Althouse, A.C.Cummings, T.L.Garrard, E.C.Stone, and R.E.Vogt, "The Voyager Cosmic Ray Instrument", ISEE Transactions on Nuclear Science, Vol. 26, 1979, pp. 513

SCIENTIFIC PAPERS

See file VOYAGER-REFERENCES in the data directory

VOL_TIME_COVERAGE: 1977-09-07 to 1992-12-31

FILE_NAMING_CONVENTION: CRS files are named according to the start time of the data contained in the file as follows: V1xx.NSSDC Here the xx stands for the two digits of the year of the data contained in the file.

FILE_TIME_COVERAGE:
Data appear as one file for each year from 1977 - 1992.

V177.NSSDC 1977 launch - 78/01/01 00:00:00

Other similarly named file sets contain each year's data starting from January 1.

/* EOF */
/* list of data quantities in order on the files follows */

SUBM_NAME: Dr. Nand Lal
SUBM_ADDR: Goddard Space Flight Center
Code 935
Greenbelt, MD 20771

Electronic mail: nand@voyager.gsfc.nasa.gov
LHEAVX::LAL
SUBM_DATE: 1994-10-07
TITLE: Format for Voyager-1 CRS Cruise Data Archive Data Set
DESCR: Format description of the Voyager-1 Cosmic Ray Subsystem cruise phase energetic particle data measurements archive data set, September 7, 1977 through 1993.
REL_DATE: 1994-10-07

RECORD_FIELD_MNEMONICS: See above in the DATA_SET_PARAMETERS for basic description of quantities.

TIME,
HELIUMFLUX1,
HELIUMFLUX2,
HELIUMFLUX3,
HELIUMFLUX4,
HELIUMFLUX5,
HELIUMFLUX6,
HELIUMFLUX7,
HELIUMFLUX8,
PROTONFLUX1,
PROTONFLUX2,
PROTONFLUX3,
PROTONFLUX4,
PROTONFLUX5,
PROTONFLUX6,
PROTONFLUX7,
PROTONFLUX8,
HELIUMFLUX9,
HELIUMFLUX10,
HELIUMFLUX11,

BRIAS .
BRIASZ3 .
BRIBSE .
BRIBSP .
BRIBSZ2 .
BRIPENL .
BRIPENH .
BRIPGL .
BRIPGH .
BRIBS4E .
BRIBS4P .
BRIBS4 .
BRIBS4Z2 .
BRIBS2E .
BRIBS2P .
BRIBS2 .
BRIBS2Z2 .
BRIBS3E .
BRIBS3P .
BRIBS3 .
BRIBS3Z2 .
BRISA1 .
BRISA2 .
BRIG1 .
BRIISA1 .
BRIISA2 .
BRIIG1 .
BRIIAS .
BRIIASZ3 .
BRIIBSE .
BRIIBSP .
BRIIBSZ2 .
BRIIPENL .
BRIIPENH .
BRIIPGL .

```
    X
  W1.W2.^D8.^GA.^GB
BRTLO          .
BRTLO          .
    X

    X
  W1.W2.D5.^D6.^GA.^GB.^UT
BRTHI          .
BRTHI          .
    X

    X
  W1.W2.D7.^D8.^GA.^GB.^UT
```

DATA_RECORD_SYNTAX: See the Description of Data segment of the DATA_SET_PARAMETER section.
Each record has terminators of the \n form.

/* EOF */

VOYAGER 2

VG2 CRS 6-HOUR CRUISE MODE DATA

77-076A-08B SPHE-00197

THIS DATASET CONSISTS OF FOUR CD'S. THE CD REPLACE THE 9 TRACK TAPES. A DIRECTORY OF THE CD AS WELL AS A COPY OF THE REFERENCE DOCUMENT HAS BEEN PLACED IN CATALOG. THE KD AND KW WILL REPLACE THE DD &DC NUMBERS TIME SPAN TIME AS FOLLOW:

KD#	KW#	TIME SPAN
KD022275	KW000179	09/07/77 -06/30/05

VOYAGER 2

VOYAGER 2 CRS 6-HOUR CRUISE DATA

77-076A-08B

THIS DATA SET CONSISTS OF 1 MAGNETIC TAPE. THE TAPE IS 9-TRACK, 6250 BPI, ASCII, CREATED ON A VAX COMPUTER WITH A LABEL NAME OF "VG-CRS". A DIRECTORY OF THE TAPE, AS WELL AS A COPY OF THE REFERENCE DOCUMENT HAVE BEEN INCLUDED IN THE CATALOG. THE D AND C NUMBER ALONG WITH ITS TIME SPAN IS LISTED BELOW.

D#	C#	FILES	TIMESPAN
D-107794	C-031720	21	08/24/77-12/31/93

Copied to CD 06/30/04

Directory of VG2-CRS 6-HR CRUISE DATA

v2HEADER.CRS;1	VY2CR78P.DAT;1	VY2CR79A.DAT;1	VY2CR79B.DAT;1
VY2CR82A.DAT;1	VY2CR82B.DAT;1	VY2CRS77.DAT;1	VY2CRS80.DAT;1
VY2CRS81.DAT;1	VY2CRS83.DAT;1	VY2CRS84.DAT;2	VY2CRS85.DAT;1
VY2CRS86.DAT;1	VY2CRS87.DAT;1	VY2CRS88.DAT;1	VY2CRS89.DAT;1
VY2CRS90.DAT;1	VY2CRS91.DAT;1	VY2CRS92.DAT;1	VY2CRS93.DAT;1
VY2CRS_REF.DOC;1			

Total of 21 files.

Header for NSSDC submission for Voyager-2 Cruise Archive
Applies to the TEXT datasets formed by program DCFLUX from the original BINARY IBM mainframe datasets.

VOL_CREATION_DATE: 1994-10-07

MEDIUM_DESCRIPTION: 1/2 inch, 9-track, 6250 bpi magnetic tape

TECHNICAL_CONTACT:
Dr. Nand Lal
Goddard Space Flight Center
Code 935
Greenbelt, MD 20771

Electronic Mail: LHEAVX::LAL
Electronic Mail: nand@voyager.gsfc.nasa.gov
Telephone: 301-286-7350

PREV_VOLS: None

DATA_SET_NAME: Voyager-2 Cruise Mode Data Archive

DATA_SOURCE: Voyager-2 Cosmic Ray Subsystem

SCIENTIFIC_CONTACT:
Dr. Frank McDonald
Institute for Physical Science and Technology
University of Maryland
College Park, MD 20742

Electronic Mail: fm27@umail.umd.edu
Telephone: 301-405-4861

SPACECRAFT_CHARACTERISTICS: Voyager-2 was launched on August 28, 1977, encountered Jupiter on July 9, 1979, Saturn on August 25, 1981, Uranus on January 24, 1986 and Neptune on August 25, 1989. It's trajectory is taking it toward the nose of the sun's heliosphere and below the ecliptic. At the end of 1992 the sun/spacecraft distance was about 39 AU, and the spacecraft direction about 27 degrees off the sun's forward motion line in the ecliptic. The spacecraft is instrumented with a full suite of magnetic field, plasma and energetic particle and cosmic ray sensors. The Imaging experiment has sent back wonderful pictures of the planets and their moons and rings.

INVESTIGATION_OBJECTIVES: This instrument is designed to exploit to the fullest practical degree the proposed trajectories of Voyagers-1 and -2. The significance of these measurements will be greatly enhanced by concurrent measurements with similar particle telescopes on satellites such as the Pioneers, IMPs, and similar series in near-earth orbits. similar series in near-earth orbits.

More pages from the data

DSC #754
77-076A-08B

Header for NSSDC submission for Voyager-2 Cruise Archive
Applies to the TEXT datasets formed by program DCFLUX from the original BINARY IBM mainframe datasets.

VOL_CREATION_DATE: 1994-10-07

MEDIUM_DESCRIPTION: 1/2 inch, 9-track, 6250 bpi magnetic tape

TECHNICAL_CONTACT:
Dr. Nand Lal
Goddard Space Flight Center
Code 935
Greenbelt, MD 20771

Electronic Mail: LHEAVX::LAL
Electronic Mail: nand@voyager.gsfc.nasa.gov
Telephone: 301-286-7350

PREV_VOLS: None

DATA_SET_NAME: Voyager-2 Cruise Mode Data Archive

DATA_SOURCE: Voyager-2 Cosmic Ray Subsystem

SCIENTIFIC_CONTACT:
Dr. Frank McDonald
Institute for Physical Science and Technology
University of Maryland
College Park, MD 20742

Electronic Mail: fm27@umail.umd.edu
Telephone: 301-405-4861

SPACECRAFT_CHARACTERISTICS: Voyager-2 was launched on August 28, 1977, encountered Jupiter on July 9, 1979, Saturn on August 25, 1981, Uranus on January 24, 1986 and Neptune on August 25, 1989. It's trajectory is taking it toward the nose of the sun's heliosphere and below the ecliptic. At the end of 1992 the sun/spacecraft distance was about 39 AU, and the spacecraft direction about 27 degrees off the sun's forward motion line in the ecliptic. The spacecraft is instrumented with a full suite of magnetic field, plasma and energetic particle and cosmic ray sensors. The Imaging experiment has sent back wonderful pictures of the planets and their moons and rings.

INVESTIGATION_OBJECTIVES: This instrument is designed to exploit to the fullest practical degree the proposed trajectories of Voyagers-1 and -2. The significance of these measurements will be greatly enhanced by concurrent measurements with similar particle telescopes on satellites such as the Pioneers, IMPs, and similar series in near-earth orbits. similar series in near-earth orbits.

The principle scientific objectives of this experiment are:

1.) To measure the flow patterns of energetic solar and galactic particles separately in the inter-planetary field. To interpret this measurement, simultaneous determination of the energy spectrum, radial gradient, distribution, and streaming parameters is required for each nuclear species and over as wide an energy range as is practicable.

2.) To measure the energy spectra, and isotopic composition of galactic and solar cosmic rays from the lowest practical energies up to ~800 MeV/nucleon and (by use of objective 1) to unfold the primary flare and interstellar spectrum.

3.) To measure the time variations of the differential energy spectra of electrons, hydrogen and helium nuclei over the corresponding energy intervals. During flare events, to obtain time histories; during quiet times, to relate gross time variations to those near earth thus deducing a spatial gradient for galactic cosmic rays.

4.) To study the energy spectra, time variations and spatial gradients associated with recurrent and non-flare associated interplanetary proton and helium streams and to define the related solar or inter-planetary acceleration processes.

5.) To provide information on the energetic particle distribution surrounding Jupiter and Saturn.

6.) To try to determine the extent of the solar cavity, the energetic particle phenomena occurring at this interface and the cosmic ray density in nearby interstellar space.

INSTRUMENT_ATTRIBUTES: The California Institute of Technology (CIT)/ Goddard Space Flight Center (GSFC) experiment on Voyager-1 and -2 (CRS) consists of three types of solid state detector telescopes, the High Energy Telescopes (HET-I and II), the Low Energy dE/dx vs. E Telescopes (LET A,B,C, and D) and The Electron Telescope (TET). The HETs and LETs are redundant and are designed to complement each other and to cover a broad range in energy, intensity, and charge spectra. Charged particle spectra are measured over energy intervals as follows:

Particle Component	Energy Range
Galactic cosmic ray protons and Solar protons	1.8 - 800 MeV
Galactic cosmic ray helium and Solar helium	1.8 - 600 MeV/nucleon
Galactic and Solar electrons	.2 - 13.0 MeV
Li,Be,B,C,N,O,F,Ne and their isotopic composition	6 MeV/nuc - 200 MeV/nuc
Integral flux of IONS > 70 MeV	

	Geometrical Factors
HET	Varies from about .74 - 1.7 depending

	if the event is A or B Stopping or Penetrating
LET	0.440 cm2-ster. (nominal)
TET	Varies from about .66 - 3.12 depending upon depth of penetration into the Di stack.

High Energy Telescope: The HET consists of a multi-element stack of solid state detectors. Particles can enter this telescope from both ends of this stack. The Two "A" elements (see diagram below) are single lithium drift detectors, 8 cm2 area and .15 mm thick. The "C1" element is a surface barrier detector 8 cm2 and 3 mm thick. Next is an array of six "C" surface barrier detectors each 8 cm2 and 6 mm thick and finally two curved 8 cm2 and 2 mm thick "B" detectors are stacked to form a two-ended telescope.

For particles which come to rest within this stack (4 - 70 MeV/ nucleon) three measurements are made: energy loss (dE/dx), total energy, and range. For particles which penetrate completely through the stack of solid state detectors three separate dE/dx measurements are made. This multiparameter analysis reduces the back-ground level of spurious events to a negligible level. Charge resolution for penetrating particles is possible up to about 200 MeV/nucleon. It is estimated that the absolute uncertainty in the helium flux is about 7% at 400 MeV and about 5% at energies below 200 MeV.

Low Energy Telescope. This detector was designed to measure low-energy solar flare particles in the interplanetary space and trapped particles in the Jovian and Saturnian magnetospheres. Its geometry factor (4.4E-01 cm**2.sr) allows measurement of fluxes as high as 5.0E+05/(cm**2.s.sr). The LET is a double dE/dx vs. E solid state detector. To enter this telescope a particle must pass through a 4 uM Aluminum collimator which helps define the geometry. Then two thin (35 microns thickness and 2.8 cm2 area) surface barrier detectors provide a double dE/dx measurement. Two thick (450 uM thickness and 4.5 cm2 area) lithium drift detectors provide another dE/dx and a total energy measurement. The LET covers the energy range 3 to 22 MeV/nucleon with charge resolution from Z=1 to 8.

The Electron Telescope. Eight solid state detectors, each 3 mm thick and 4.5 cm2 in area are used individually and in coincidence as total absorption spectrometers. Varying depths of tungsten absorber are between each Di element.

For more information, refer to the document:

D.E.Stillwell, W.D.Davis, R.M.Joyce, F.B.McDonald, J.H.Trainor, W.E.Althouse, A.C.Cummings, T.L.Garrard, E.C.Stone, and R.E.Vogt, "The Voyager Cosmic Ray Instrument", ISEE Transactions on Nuclear Science, Vol. 26, 1979, pp. 513

DATA_SET_PARAMETERS:

Time of start of averaging interval in seconds from start of base year, TIME;

6 hour averages of the following fluxes, plus statistical errors units of particles/(cm**2.sec.ster.MeV/nuc) HELIUMFLUXi or PROTONFLUXi ;

6 hour averages of the following rates, plus statistical errors units of particles/second;

The following diagrams are given to assist the user in understanding the meaning of the data quantities present.

Simplistic diagram of Voyager instruments:

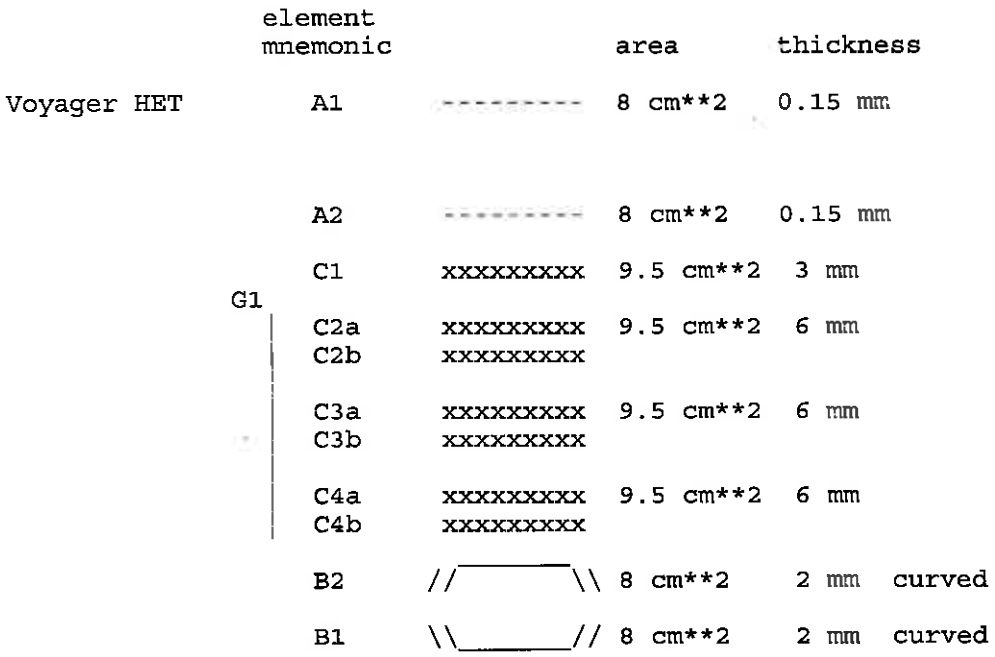

	element mnemonic	area	thickness
Voyager LET	**********		4uM AL collimator light baffle
	L1 ---------	2.8 cm**2	surface barrier 35 uM
	L2 ---------	2.8 cm**2	surface barrier 35 uM
	L3 xxxxxxxxx	4.5 cm**2	surface barrier 450 uM
	L4 xxxxxxxxx	4.5 cm**2	surface barrier 450 uM
Voyager TET	D1 xxxxxxxxx		
	D2 xxxxxxxxx		.25 mm tungsten absorber
	D3 xxxxxxxxx		.56 mm tungsten absorber
	D4 xxxxxxxxx		1.12 mm tungsten absorber
	D5 xxxxxxxxx		1.60 mm tungsten absorber
	D6 xxxxxxxxx		2.03 mm tungsten absorber
	D7 xxxxxxxxx		2.34 mm tungsten absorber
	D8 xxxxxxxxx		

Di detectors= 4.5 cm**2 Lithium drifted 3mm
tungsten absorbers are 18.0 g/cm**3

where cm = centimeters
mm = millimeter
where uM = micrometer

Data present on our tape(s) :
For Voyager-2:
Because of changes in instrument status the Cruise submission was divided into 3 general sections. Each of these sections has slightly different data quantities which will be available or not available. These periods are as follows:
1) Launch - June 29, 1979 (pre-Jupiter encounter)

2) 8/22/79 (~post Jupiter) - 4/22/82
3) 4/22/82 - end of 1992
Especially in the second section, users will see quantities present which may then disappear, and later come back. Status cycling and testing are happening during this section. It was felt that extensive editing of the NSSDC submission to include only data being measured for only the times it was measured would be time consuming and confusing, and instead we have provided general indications of when this is happening. Users needing more detailed data on instrument performance are urged to contact the technical representative mentioned above.

Lists of exact data quantities we have allowed for within each of the 3 time periods are given below in the RECORD_FIELD_MNEMONICS section.
Data is segmented into yearly datasets, except for 1979 and 1982, where our time period breaks occur.

For each general dataset, quantities present are,
- Time in seconds from start of base year, for start of averaging interval

- Particle fluxes given in units particles/(cm**2.s.sr.Mev/n)
- error in the Particle flux quantity
- Rates given in units particles/s
- error in the Rate quantity

where cm = centimeters
s = second
sr = steradian

Underneath the flux designations, HELIUMFLUX1, for example, is a mnemonic code, such as M IIA2, indicating from which calibration response table this data came. It is for documenting purposes only.

The following is a description of our mnemonic naming convention for the potential fluxes and rates present on our tapes if all data quantities were present for the cruise lifetime:

In the following, the phrases "2 dimensional analysis" or "3 dimensional analysis" refer to events whose analysis utilized pulse height data from either 2 or 3 pulse height values associated with the particular event type (detector element coincidence requirement) being measured at the time. As an example, for A side events, particles enter the HET telescope from the A end, and 1) stop in A1 or A2 for 2-dimensional A stopping events
2) stop in the C123 stack for 3-dimensional A stopping events
3) pass entirely through the SumC stack and have a B1 or B2 pulse height as well and are called 3-dimensional A penetrating events.

HET fluxes :

HELIUMFLUX1	Helium4 flux in particles/cm**2.s.sr.Mev/n
M IA2	A-stopping 2 dimensional analysis, high gain data from HET-I

	4.2 - 6.0 MeV/nucleon energy range
HELIUMFLUX2 M IA3	Helium4 flux as above, A-stopping, 3 dimensional analysis, high gain data from HET-I 6.0 - 42.0 MeV/n energy range,
HELIUMFLUX3 M IL2	B-stopping 2 dimensional analysis, low gain HET-I 17.0 - 27.0 MeV/n
HELIUMFLUX4 M IL3	B-stopping 3 dimensional analysis, low gain HET-I 30.0 - 69.0 MeV/n
HELIUMFLUX5 M IB2	B-stopping 2 dimensional analysis, high gain HET-I 17.0 - 27.0 MeV/n
HELIUMFLUX6 M IB3	B-stopping 3 dimensional analysis, high gain data from HET-I 30.0 - 69.0 MeV/n
HELIUMFLUX7 M IP	B-penetrating 3 dimensional analysis, low gain penetrating data from HET-I 193.125 - 480.5 MeV/n
HELIUMFLUX8 M IPH	B-penetrating 3 dimensional analysis, high gain penetrating data from HET-I 191.925 - 475.7 MeV/n energy range
PROTONFLUX1 M IA2	Proton flux in particles/cm**2.s.sr.MeV/n A-stopping 2 dimensional analysis, high gain data from HET-I 4.2 - 6.0 MeV energy range
PROTONFLUX2 M IA3	Proton flux in particles/cm**2.s.sr.MeV/n 3 dimensional analysis, high gain data from HET-I 6.0 - 42.0 MeV energy range,
PROTONFLUX3 M IB2	B-stopping 2 dimensional analysis, high gain data from HET-I 17.0 - 27.0 MeV energy range
PROTONFLUX4 M IB3	B-stopping 3 dimensional analysis, high gain data from HET-I 30.0 - 69.0 MeV energy range
PROTONFLUX5 M IPH	B-penetrating 3 dimensional analysis, high gain penetrating data from HET-I 132.834 - 241.963 MeV energy range
HELIUMFLUX9 M IIA2	Helium4 flux in particles/cm**2.s.sr.Mev/n A-stopping 2 dimensional analysis, high gain data from HET-II 4.2 - 6.0 MeV/n energy range
HELIUMFLUX10	Helium4 flux as above, A-stopping,

M IIA3	3 dimensional analysis, high gain data from HET-II 6.0 - 42.0 MeV/n energy range,
HELIUMFLUX11 M IIL2	B-stopping 2 dimensional analysis, low gain HET-II 17.0 - 27.0 MeV/n
HELIUMFLUX12 M IIL3	B-stopping 3 dimensional analysis, low gain HET-II 30.0 - 69.0 MeV/n
HELIUMFLUX13 M IIE2	B-stopping 2 dimensional analysis, high gain HET-II 17.0 - 27.0 MeV/n
HELIUMFLUX14 M IIE3	B-stopping 3 dimensional analysis, high gain data from HET-II 30.0 - 69.0 MeV/n
HELIUMFLUX15 M IIP	B-penetrating 3 dimensional analysis, low gain penetrating data from HET-II 193.125 - 480.486 MeV/n
HELIUMFLUX16 M IIPH	B-penetrating 3 dimensional analysis, high gain penetrating data from HET-II 191.925 - 475.705 MeV/n energy range
PROTONFLUX6 M IIA2	Proton flux in particles/cm**2.s.sr.MeV/n A-stopping 2 dimensional analysis, high gain data from HET-II 4.2 - 6.0 MeV energy range
PROTONFLUX7 M IIA3	Proton flux in particles/cm**2.s.sr.MeV/n 3 dimensional analysis, high gain data from HET-II 6.0 - 42.0 MeV energy range,
PROTONFLUX8 M IIE2	B-stopping 2 dimensional analysis, high gain data from HET-II 17.0 - 27.0 MeV energy range
PROTONFLUX9 M IIB3	B-stopping 3 dimensional analysis, high gain data from HET-II 30.0 - 69.0 MeV energy range
PROTONFLUX10 M IIPH	B-penetrating 3 dimensional analysis, high gain penetrating data from HET-II 132.834 - 241.963 MeV energy range
LET fluxes : (all stopping particle events)	
PROTONFLUX11 M LA2	Proton 2-dimensional analysis from LET-A energy range of 1.8 - 3.3 MeV
PROTONFLUX12 M LB2	Proton 2-dimensional analysis from LET-B energy range of 1.8 - 3.3 MeV

```
-----------------------------------
PROTONFLUX13              Proton 2-dimensional analysis from LET-C
M LC2                       energy range of 1.8 - 3.3 MeV
-----------------------------------
PROTONFLUX14              Proton 2-dimensional analysis from LET-D
M LD2                       energy range of 1.8 - 3.3 MeV
-----------------------------------
PROTONFLUX15              Proton 3-dimensional analysis from LET-A
M LA3                       energy range of 3.25 - 8.1 MeV
-----------------------------------
PROTONFLUX16              Proton 3-dimensional analysis from LET-B
M LB3                       energy range of 3.25 - 8.1 MeV
-----------------------------------
PROTONFLUX17              Proton 3-dimensional analysis from LET-C
M LC3                       energy range of 3.25 - 8.1 MeV
-----------------------------------
PROTONFLUX18              Proton 3-dimensional analysis from LET-D
M LD3                       energy range of 3.25 - 8.1 MeV
-----------------------------------
-----------------------------------
HELIUMFLUX17               Helium4 2-dimensional analysis from LET-A
M LA2                      1.800 - 2.800 MeV/n energy range
-----------------------------------
HELIUMFLUX18               Helium4 2-dimensional analysis from LET-B
M LB2                      1.800 - 2.800 MeV/n energy range
-----------------------------------
HELIUMFLUX19               Helium4 2-dimensional analysis from LET-C
M LC2                      1.800 - 2.800 MeV/n energy range
-----------------------------------
HELIUMFLUX20               Helium4 2-dimensional analysis from LET-D
M LD2                      1.800 - 2.800 MeV/n energy range
-----------------------------------
HELIUMFLUX21               Helium4 3-dimensional analysis from LET-A
M LA3                      2.800 - 8.000 MeV/n energy range
-----------------------------------
HELIUMFLUX22               Helium4 3-dimensional analysis from LET-B
M LB3                      2.800 - 8.000 MeV/n energy range
-----------------------------------
HELIUMFLUX23               Helium4 3-dimensional analysis from LET-C
M LC3                      2.800 - 8.000 MeV/n energy range
-----------------------------------
HELIUMFLUX24               Helium4 3-dimensional analysis from LET-D
M LD3                      2.800 - 8.000 MeV/n energy range
-----------------------------------
-----------------------------------
HET   event type RATES (for flux calculations) :
-----------------------------------
*   NOMINAL COINCIDENCE CONDITION status
*   exists unless otherwise noted.
*   To interpret the LOGIC EQUATIONS (refer to simplistic telescope
*   diagrams above) :  EXAMPLE:  BRIBSP (the BR pre-mnemonic
*   indicates to our system a rate bin request and is left here for
*   documentation purposes only)
*              B1.B2.^SB.^C1.^G1.^A2
*   The above LOGIC EQUATION means: a particle entered the
*   telescope from the B end, and met the coincidence condition of
*   passing through B1, stopping in either B2 or the C432 stack,
*   but NOT (= ^ ) tripping the Slant threshold condition SB,
*   NOT going into C1, Guard G1, or A2.
```

```
---------------------------------
PROTONFLUX13              Proton 2-dimensional analysis from LET-C
M LC2                       energy range of 1.8 - 3.3 MeV
---------------------------------
PROTONFLUX14              Proton 2-dimensional analysis from LET-D
M LD2                       energy range of 1.8 - 3.3 MeV
---------------------------------
PROTONFLUX15              Proton 3-dimensional analysis from LET-A
M LA3                       energy range of 3.25 - 8.1 MeV
---------------------------------
PROTONFLUX16              Proton 3-dimensional analysis from LET-B
M LB3                       energy range of 3.25 - 8.1 MeV
---------------------------------
PROTONFLUX17              Proton 3-dimensional analysis from LET-C
M LC3                       energy range of 3.25 - 8.1 MeV
---------------------------------
PROTONFLUX18              Proton 3-dimensional analysis from LET-D
M LD3                       energy range of 3.25 - 8.1 MeV
---------------------------------
---------------------------------
HELIUMFLUX17               Helium4 2-dimensional analysis from LET-A
M LA2                      1.800 - 2.800 MeV/n energy range
---------------------------------
HELIUMFLUX18               Helium4 2-dimensional analysis from LET-B
M LB2                      1.800 - 2.800 MeV/n energy range
---------------------------------
HELIUMFLUX19               Helium4 2-dimensional analysis from LET-C
M LC2                      1.800 - 2.800 MeV/n energy range
---------------------------------
HELIUMFLUX20               Helium4 2-dimensional analysis from LET-D
M LD2                      1.800 - 2.800 MeV/n energy range
---------------------------------
HELIUMFLUX21               Helium4 3-dimensional analysis from LET-A
M LA3                      2.800 - 8.000 MeV/n energy range
---------------------------------
HELIUMFLUX22               Helium4 3-dimensional analysis from LET-B
M LB3                      2.800 - 8.000 MeV/n energy range
---------------------------------
HELIUMFLUX23               Helium4 3-dimensional analysis from LET-C
M LC3                      2.800 - 8.000 MeV/n energy range
---------------------------------
HELIUMFLUX24               Helium4 3-dimensional analysis from LET-D
M LD3                      2.800 - 8.000 MeV/n energy range
---------------------------------
---------------------------------
HET   event type RATES (for flux calculations) :
---------------------------------
*   NOMINAL COINCIDENCE CONDITION status
*   exists unless otherwise noted.
*   To interpret the LOGIC EQUATIONS (refer to simplistic telescope
*   diagrams above) :  EXAMPLE:  BRIBSP (the BR pre-mnemonic
*   indicates to our system a rate bin request and is left here for
*   documentation purposes only)
*              B1.B2.^SB.^C1.^G1.^A2
*   The above LOGIC EQUATION means: a particle entered the
*   telescope from the B end, and met the coincidence condition of
*   passing through B1, stopping in either B2 or the C432 stack,
*   but NOT (= ^ ) tripping the Slant threshold condition SB,
*   NOT going into C1, Guard G1, or A2.
```

```
*
---------------------------------
HET-I event type rates (for flux calculations) :
---------------------------------
BRIAS                          A-Stopping High Gain
  A1.A2.^C4.^G1.^B2

BRIASZ3                        A-Stopping Low Gain  Atomic Number
                                    Z >= 3
  A1.A2.SA.^C4.^G3.^B2

BRIBSE                         B-Stopping electron event
  B1.B2.C4.^SB.^C1.^G1.^A2

BRIBSP                         B-Stopping High Gain
  B1.B2.SB.^C1.^G1.^A2

BRIBSZ2                        B-Stopping Low Gain  Atomic Number
                                                Z >= 2
  B1.B2.SB.^C1.^G3.^A2

BRIPENH                        B-Penetrating High Gain
  B1.B2.C1

BRIPENL                        B-Penetrating Low Gain
  B1.B2.C1

BRIPGH                         Guard High Gain
  B1.B2.C1.^G1

BRIPGL                         Guard Low Gain
  B1.B2.C1.^G1

BRIBS4E
  B1.B2.C4.^C3.^SB.^G1         Stop in C4, did NOT get into C3

BRIBS4P
  B1.B2.C4.^C3.SB.^G1                "                          , High
                                                                  Gain

BRIBS4
  B1.B2.C4.^C3.^SB.^G1               "

BRIBS4Z2
  B1.B2.C4.^C3.SB.^G1                "                          , Low
                                                                  Gain

BRIBS3E
  B1.B2.C4.C3.^C2.^SB.^G1      Stop in C3, did NOT get into C2, High
                                                                  Gain

BRIBS3P
  B1.B2.C4.C3.^C2.SB.^G1             "

BRIBS3
  B1.B2.C4.C3.^C2.^SB.^G1            "

BRIBS3Z2
  B1.B2.C4.C3.^C2.SB.^G1             "                          , Low
```

Gain

BRIBS2E
  B1.B2.C4.C3.C2.^C1.^SB.^G1 Stop in C2, did NOT get into C1, High Gain

BRIBS2P
  B1.B2.C4.C3.C2.^C1.SB.^G1 "

BRIBS2
  B1.B2.C4.C3.C2.^C1.^SB.^G1 "

BRIBS2Z2
  B1.B2.C4.C3.C2.^C1.SB.^G1 " , Low Gain

HET-II event type RATES (for flux calculations) :
  interpreted analagously to HET-I

BRIIAS
  A1.A2.^C4.^G1.^B2

BRIIASZ3
  A1.A2.SA.^C4.^G3.^B2

BRIIBSE
  B1.B2.C4.^SB.^C1.^G1.^A2

BRIIBSP
  B1.B2.SB.^C1.^G1.^A2

BRIIBSZ2
  B1.B2.SB.^C1.^G3.^A2

BRIIPENH
  B1.B2.C1

BRIIPENL
  B1.B2.C1

BRIIPGH
  B1.B2.C1.^G1

BRIIPGL
  B1.B2.C1.^G1

BRIIBS4E
  B1.B2.C4.^C3.^SB.^G1

BRIIBS4P
  B1.B2.C4.^C3.SB.^G1

BRIIBS4
  B1.B2.C4.^C3.^SB.^G1

BRIIBS4Z2
  B1.B2.C4.^C3.SB.^G1

```
BRIIBS3E
  B1.B2.C4.C3.^C2.^SB.^G1

BRIIBS3P
  B1.B2.C4.C3.^C2.SB.^G1

BRIIBS3
  B1.B2.C4.C3.^C2.^SB.^G1

BRIIBS3Z2
  B1.B2.C4.C3.^C2.SB.^G1

BRIIBS2E
  B1.B2.C4.C3.C2.^C1.^SB.^G1

BRIIBS2P
  B1.B2.C4.C3.C2.^C1.SB.^G1

BRIIBS2
  B1.B2.C4.C3.C2.^C1.^SB.^G1

BRIIBS2Z2
  B1.B2.C4.C3.C2.^C1.SB.^G1

-----------------------------------
HET-I singles rates
-----------------------------------
BRIA1H                      Singles rate, high gain, for the A1
  A1                           element
                            below are all high gain until noted
BRIA2H
  A2

BRIC1H
  C1

BRIC2H
  C2

BRIB1H
  B1

BRISBH
  SB

BRIC3H
  C3

BRIC4H
  C4

BRIB2H
  B2

BRIG1
  G1

BRIA1L                    begin low gain singles here
  A1
```

BRIA2L
  A2

BRIC1L
  C1

BRIC2L
  C2

BRIB1L
  B1

BRISA1
  SA

BRISA2
  SA

BRISBL
  SB

BRIC3L
  C3

BRIC4L
  C4

BRIB2L
  B2

HET-II singles rates
  Interpreted the same as HET-I singles rates

BRIIA1H
  A1

BRIIA2H
  A2

BRIIC1H
  C1

BRIIC2H
  C2

BRIIB1H
  B1

BRIISBH
  SB

BRIIC3H
  C3

BRIIC4H
  C4

```
BRIIB2H
  B2

BRIIG1
  G1

BRIIA1L                    begin low gain singles here
  A1

BRIIA2L
  A2
BRIIC1L
  C1

BRIIC2L
  C2

BRIIB1L
  B1


BRIISA1
  SA

BRIISA2
  SA

BRIISBL
  SB

BRIIC3L
  C3

BRIIC4L
  C4

BRIIB2L
  B2

-----------------------------------
LET singles rates  in high gain
-----------------------------------
BRLA1
  L1

BRLA2
  L2

BRLA3
  L3

BRLA4
  L4

BRSLA
  SL

BRSLB
  SL
```

BRLB1
  L1

BRLB2
  L2

BRLB3
  L3

BRLB4
  L4

BRLC1
  L1

BRLC2
  L2

BRLC3
  L3

BRLC4
  L4

BRSLD
  SL

BRLD1
  L1

BRLD2
  L2

BRLD3
  L3

BRLD4
  L4

TET singles rates H or L at end of rate indicates High or Low Gain

---

BRD6L
  D6

BRGA+GB
  GA.GB

BRD5H
  D5

BRD7L
  D7

BRD6H
  D6
BRD7H

```
  D7

BRD5L
  D5

BRD8L
  D8

BRD1H
  D1

BRD4H
  D4

BRD2L
  D2

BRD3L
  D3

BRD1L
  D1

BRD3H
  D3

BRD2H
  D2

BRD4L
  D4

*  MAJOR STATUS CHANGE CONFIGURATIONS IN CRUISE AFFECT THESE
----------------------------------
LET event type rates (for flux calculations) :
----------------------------------
BRLATRP
  L1.L2.^L4

BRLBTRP
  L1.L2.^L4

BRLCTRP
  L1.L2.L3.^L4

BRLCTRP
  L1.L2.^L4

BRLDTRP
  L1.L2.^L4

BRLC                        High Gain  (typical mnemonic)
  L1.L2.L3.^SL.^L4
BRLC
  L1.L2.^SL.^L4

BRLCZ3                      Low Gain  Atomic Number Z >= 3
  L1.L2.L3.SL.^L4                (typical mnemonic)
```

```
BRLCZ3
  L1.L2.SL.^L4

BRLD
  L1.L2.L3.^SL.^L4

BRLD
  L1.L2.^SL.^L4

BRLDZ3
  L1.L2.L3.SL.^L4

BRLDZ3
  L1.L2.SL.^L4

BRLA
  L1.L2.^SL.^L4

BRLAZ3
  L1.L2.SL.^L4

BRLB
  L1.L2.^SL.^L4

BRLBZ3
  L1.L2.SL.^L4

-----------------------------------
TET event type rates (for flux calculations) :
-----------------------------------
BRTAN
  W1.W2.D3.^D8.^GA.^GB

BRTAN
  W1.W2.^D8.^GA.^GB

BRTLO
  W1.W2.D3.D5.^D6.^GA.^GB.^UT

BRTLO
  W1.W2.D5.^D6.^GA.^GB.^UT

BRTHI
  W1.W2.D3.D7.^D8.^GA.^GB.^UT

BRTHI
  W1.W2.D7.^D8.^GA.^GB.^UT
```

Description of DATA

Files of data are in ASCII text format, variable length formatted records, readable by the example program given below. The records of these datasets contain words with information on start time, data quantities are present, the averaging interval , and ASCII character data descriptions of the specific coincidence logic condition which gives rise to the data quantity being presented.

If the Error value is -1.0, data for this item is not available. If the Flux and Error are 0.0 no events occurred during the collection time.

The format of the text data is generally as follows:

Record #:	general length	description
1	C*12	Satellite name
2	C*n	Start time of first 6 hour average present
3	C*n	Stop time of last 6 hour average present
4	C*3	Number of bins (data quantities present)

Records 5-(N+4) (where N = number of bins): Bin Label Records

C*3	bin number
C*n	Character data label description

Records N+4- ... Data records:

C*19	Start time as yy-mm-ddThh:mm:ss
C*15	Value of data quantity 1
C*15	Error in data quantity 1
.	.
.	.
C*15	Value of data quantity N
C*15	Error in data quantity N

This program will list the contents of the data for one quantity.

```
C       EXTRACTS SPECIFIED ITEM FROM A VOYAGER NSSDC FORMATTED FILE
        IMPLICIT NONE
        CHARACTER*12 SATID
        CHARACTER*19 START,END,T
        CHARACTER*132 LABEL
        CHARACTER*100 FMTSTRING
        CHARACTER*40 FNAME
        INTEGER I,IBIN,NOBINS
        REAL FLUX,ERROR
        WRITE (6,*) 'FILE:'
        READ(5,'((A))') FNAME
        OPEN(UNIT=1,FILE=FNAME,STATUS='OLD')
        READ(1,'((A))') SATID
        WRITE(6,'((A))') SATID
        READ(1,'((A))') START
        WRITE(6,'((A))') START
        READ(1,'((A))') END
        WRITE(6,'((A))') END
        READ(1,*) NOBINS
        WRITE(6,*) 'BIN NUMBER:'
        READ(5,*) IBIN
        IF ((IBIN .LT. 1) .OR. (IBIN .GT. NOBINS)) THEN
```

```
            WRITE(6,*) 'BIN # ',IBIN,' NOT IN RANGE (1,',NOBINS,').'
                STOP
         ENDIF
         WRITE(FMTSTRING,1) 2*(IBIN-1)*15
1        FORMAT('((A),',I5,'X,2E15.5)')
         DO 10 I=1,IBIN-1
            READ(1,'((A))') LABEL
10       CONTINUE

         READ(1,'((A))') LABEL
         WRITE(6,*) LABEL

         DO 20 I=IBIN+1,NOBINS
            READ(1,'((A))') LABEL
20       CONTINUE

         DO 30 I=1,1000000
            READ(1,FMTSTRING,END=100) T,FLUX,ERROR
            WRITE(6,25) T,FLUX,ERROR
25          FORMAT(1X,A19,1X,2E15.5)
30       CONTINUE
         STOP
100      WRITE(6,*) 'END OF FILE'
         STOP
         END
```

DATA_SET_QUALITY/INSTRUMENT_PERFORMANCE:

Five status configurations have been used in the CRUISE portions of the mission (see below).

The LET and TET are in non-nominal status states for much of the CRUISE portion of the mission. To access non-nominal rate data in our system requires input to our FLUXPLOT program (which makes data summaries) of the exact COINCIDENCE LOGIC EQUATION described by the non-nominal instrument status. To handle both nominal and non-nominal times we have requested both states for the lifetime cruise periods. Therefore, users of this NSSDC data need to be aware of the correct status condition for times of interest, and look at the corresponding data quantity for our submission, in order not to be confused by thinking there is no data for those quantities affected.

The exact order of data on our tapes is listed after the REFERENCES section of this header information.

VOYAGER-2 CRUISE PERIODS (NON-ENCOUNTER) STATUS SUMMARIES

Telescope nominal conditions are indicated by a 00 in the right-most byte of each status word for words 5 - 10 (05 - 0A in the left byte of each status word).

```
VOLUME time
------ ----
28493  10/24/77 19:00:0   IN CONFIG (1)
 STATUS CONFIG (1) = NOMINAL + 0020 0580 0680 0780 0880      0D0A
83048   5/16/79  1:45:0   IN CONFIG (2)
 STATUS CONFIG (2) = NOMINAL + 0020 0580 0680 0780 0880 0A04 0D0A
98567  10/24/79 17:30:0   IN CONFIG (3)
 STATUS CONFIG (3) = NOM + 0020 0308 0580 0680 0780 0880 0A04 0D04
159943  7/25/81  1:30:0   IN CONFIG (4)
 STATUS CONFIG (4) = NOM + 0020 0308 0582 0680 0700 0880 0A04 0D04
287282  3/12/85 12:15:0   in config (5)
 STATUS CONFIG (5) = NOM + 0020 0308 0582 0680 0700 0880 0A00 0D04


 status byte meanings:
   0020    High Volt. enable indicator
   0308    LB1 power off
   0580    delete LA3 terms
   0582    delete LA3 terms, disable LET B
   0600    nominal
   0680    delete LC3 terms
   0780    delete LB3 terms
   0880    delete LD3 terms
   0A00    nominal
   0A04    delete  D3 terms
   0D04    Het 1 gain set high
   0D0A    Het 1 and Het 2 auto gain flag on

other status bytes seen sometimes below:
   08A0    Het 2 delete C1 and B1 terms
   0D05    Het 1 and Het 2 gain set high
   0583    disable LET A, disable LET B   PHA analysis


EXCLUDES FROM STATUS LISTS AND STANDARD DATA SPIKE/ BAD DATA LISTS:

      WORD 0 CHANGE AT 37779  1/29/78 12:30:0   0762
      WORD 0 CHANGE AT 48894  5/25/78  7:15:0   03A0
      WORD 0 CHANGE AT 50932  6/15/78 12:45:0   0A20

      CYCLING OF SOME STATUS WORDS FOR 80334 - 80436
                           4/17/79 19:15:0 - 4/18/79 20:45:0

      CYCLING OF SOME STATUS WORDS FOR 92527 - 98566
                           8/22/79 19:30:0 - 10/24/79 17:15:0

      CYCLING OF MOST STATUS WORDS FOR 159931 - 159943
                           7/24/81 22:30:0 -  7/25/81  1:30:0

      Word 0 change at 184751  4/ 9/82 11:30:0 - 19:00  0A60


      FROM ~315645 -  315658 VARIOUS CYCLING AS FOR ENCOUNTER
             1/1/86 23:00:00 - 1/2/86 2:15:00

      ENCOUNTER CYCLING 437444 -  437459
                           6/23/89 16:45:0 - 20:30:0

      WORD 0 CHANGE  AT 517068 10/01/91  2:45:0   0DA7
```

excluded data times (+localized and non-localized data blips):
These times have been excluded from our NSSDC data:

S VOYAGER-2

SI		77/09/18	00:00:00	77/12/31 00:00:00
SE		77/09/18	00:00:00	77/10/07 00:00:00
SE		77/10/10	00:00:00	77/10/11 00:00:00
SE		77/10/12	00:00:00	77/10/15 00:00:00
SE		77/10/18	00:00:00	77/10/19 00:00:00
SE		77/11/22	00:00:00	77/12/03 00:00:00
SE		77/12/27	00:00:00	77/12/29 00:00:00
SI		78/01/01	00:00:00	78/12/31 00:00:00
SE	*	78/01/29	12:30:00	78/01/29 17:30:00
SE		78/04/08	00:00:00	78/05/25 00:00:00
SE	*	78/05/25	07:15:00	78/05/25 07:30:00
SE	*	78/05/27	03:15:00	78/05/27 07:15:00
SE		78/06/01	00:00:00	78/06/15 00:00:00
SE	*	78/06/15	12:45:00	78/06/15 13:00:00
SE		78/06/16	06:45:00	78/06/16 07:00:00
SE		78/06/19	01:45:00	78/06/19 02:00:00
SE		78/06/20	06:00:00	78/06/20 06:15:00
SE		78/06/22	00:30:00	78/06/22 00:45:00
SE		78/06/22	01:45:00	78/06/22 02:00:00
SE		78/06/22	02:45:00	78/06/22 03:00:00
SE		78/06/24	00:00:00	78/07/03 00:00:00
SE		78/07/13	00:00:00	78/07/23 00:00:00
SE		78/07/27	17:15:00	78/07/27 17:30:00
SE		78/11/23	21:15:00	78/11/23 21:30:00
SI		79/01/01	00:00:00	79/12/31 00:00:00
SE	*	79/04/17	19:15:00	79/04/18 20:45:00
SE		79/06/15	00:00:00	79/06/16 00:00:00
SE		79/06/29	00:00:00	79/10/24 17:15:00
SI		80/01/01	00:00:00	80/12/30 00:00:00
SI		81/01/01	00:00:00	81/12/31 00:00:00
SE		81/02/09	00:00:00	81/02/10 00:00:00
SE	*	81/07/24	22:30:00	81/07/25 01:30:00
SE		81/08/15	00:00:00	81/09/03 00:00:00
SI		82/01/01	00:00:00	82/12/31 00:00:00
SE	*	82/04/09	11:30:00	82/04/09 19:00:00
SI		83/01/01	00:00:00	83/12/31 00:00:00
SI		84/01/01	00:00:00	84/12/30 00:00:00
SI		85/01/01	00:00:00	85/12/31 00:00:00
SE		85/08/22	00:00:00	85/08/23 00:00:00
SE		85/12/12	18:00:00	85/12/13 04:00:00
SI		86/01/01	00:00:00	86/12/31 00:00:00
SE	*	86/01/01	23:00:00	86/01/02 02:15:00
SE		86/01/10	00:00:00	86/01/11 00:00:00
SE		86/01/17	00:00:00	86/01/26 06:00:00
SE		86/02/05	00:00:00	86/02/06 00:00:00
SE		86/09/23	04:00:00	86/09/23 09:00:00
SE		86/12/05	08:00:00	86/12/05 12:00:00
SI		87/01/01	00:00:00	87/12/31 00:00:00
SE		87/02/06	23:00:00	87/02/07 01:00:00
SE		87/05/07	05:00:00	87/05/07 07:00:00
SE		87/09/18	20:00:00	87/09/19 01:00:00
SE		87/11/17	01:00:00	87/11/17 04:00:00

```
SE        87/12/15 02:00:00 87/12/15 04:00:00
SI        88/01/01 00:00:00 88/12/30 00:00:00
SE        88/01/18 17:00:00 88/01/18 21:00:00
SE        88/06/18 12:00:00 88/06/18 14:00:00
SE        88/06/18 23:00:00 88/06/19 02:00:00
SE        88/06/24 04:00:00 88/06/24 06:00:00
SE        88/07/01 17:00:00 88/07/01 18:00:00
SE        88/07/09 04:00:00 88/07/09 05:00:00
SE        88/10/26 13:00:00 88/10/26 15:00:00
SI        88/01/01 00:00:00 88/12/30 00:00:00
SE        88/01/18 17:00:00 88/01/18 21:00:00
SE        88/06/18 12:00:00 88/06/18 14:00:00
SE        88/06/18 23:00:00 88/06/19 02:00:00
SE        88/06/24 04:00:00 88/06/24 06:00:00
SE        88/07/01 17:00:00 88/07/01 18:00:00
SE        88/07/09 04:00:00 88/07/09 05:00:00
SE        88/10/26 13:00:00 88/10/26 15:00:00
SI        89/01/01 00:00:00 89/12/31 00:00:00
SE  *     89/06/23 16:45:00 89/06/23 20:30:00
SE  -     89/06/23 00:00:00 89/06/24 00:00:00
SE        89/08/15 00:00:00 89/08/30 00:00:00
SI        90/01/01 00:00:00 90/12/31 00:00:00
SE        90/07/01 08:00:00 90/07/02 12:00:00
SE        90/07/26 10:00:00 90/07/27 11:00:00
SE        90/10/24 00:00:00 90/10/25 00:00:00
SE        90/10/27 00:00:00 90/10/28 00:00:00
SE        90/11/13 00:00:00 90/11/14 00:00:00
SE        90/11/19 00:00:00 90/11/20 00:00:00
SE        90/12/08 00:00:00 90/12/09 00:00:00
SE        90/12/16 00:00:00 90/12/17 00:00:00
SE        90/12/23 00:00:00 90/12/24 00:00:00
SI        91/01/01 00:00:00 91/12/31 00:00:00
SE  *     91/10/01 02:45:00 91/10/01 03:00:00
SI        92/01/01 00:00:00 92/12/30 00:00:00

*  indicates an exclude derived from the status lists


     Whole single exclude days are probably data blips which
     were never localized.



V2 encounters closest approach times:
 Jupiter     9Jul79
 Saturn     25Aug81
 Uranus     24Jan86
 Neptune    25Aug89

-----------------------------------------------------------------

Year timeline summary
Instrument condition /general health observations:


   TAN event type rates need special coincidence equations
    during part of cruise:  for TAN,  TLO,  THI
    delete the D3 term from
```

5/16/79 01:45 - 3/12/85 12:15
LET event type rates need special coincidence equations
during cruise: for LA, LC, LD high and low gains:
delete the L3 term throughout the mission

1977 Status Configuration varies from nominal at launch
Status Configuration 1 begins at 10/24/77 19:00

1978 day 98 - 210 bad times;

1979 9Jul79 Jupiter;
Status Configuration 2 begins at 5/16/79 01:45
Status Configuration 3 begins at 10/24/79 17:30
** note ** Het I gain set high also means
Het II is gain set low

1980

1981 25Aug81 Saturn
Status Configuration 4 begins at 7/25/81 01:30

1982

1983

1984

1985 Status Configuration 5 begins at 3/12/85 12:15

1986 24Jan86 Uranus

1987

1988

1989 25Aug89 Neptune

1990

1991

1992

Dr. A. Cummings (Principle Investigator, CIT) has provided the following information from the theses indicated, to summarize instrument health and experiment problems.

START OF THESIS INFORMATION ----------
From the Rick Cook thesis-

Appendix B Problems

B.1 LET B of Voyager-1

The response of this telescope was unusual in that (1) the HE mass measurement, M1, showed a relatively large energy and time dependence, (2) a relatively large 'background' of events was present in the charge range near fluorine, and (3) the L1 versus L2+L3 element tracks had an uncharacteristically blurred appearance. The problem may be electronic instability, but was not investigated in detail; instead the data from this telescope were excluded from use in the measurements presented in Chapter 4, Tables 4.1 through 4.12.

B.2 LET C of Voyager-2

On April 1, 1978 the L1 detector of this telescope experienced a simultaneous shift in energy calibration and increase in count rate, perhaps as the result of a light leak in the thin AL entrance window. Subsequent data from this telescope were not used in the measurements of Chapter 4, Tables 4.1 through 4.12.

B.3 Pulse Height Multiplication in the LET 35 um Detectors

A background effect specific to the iron group nuclei was identified in Sections 3.3 and 3.5 and necessitated the further study and special handling which is discussed here. The affected PHA events were clearly seen in Figure 3.7, a plot of the charge measurements Z1 versus Z2, as a clump of points near (Z1=26, Z2=28). Inspection of the L1, L2 and L3 pulse heights of the events in this clump revealed a very specific signature:

(1) The events lie directly on the L1 versus L3 track for iron, but lie just above the L2 versus L3 iron track, indicating that the L1 and L3 pulse heights are normal, but that the L2 pulse height is abnormally large.

(2) The events have relatively small L3 pulse heights (E{L3} less than about 170 MeV), indicating that the nuclei responsible for the events just barely penetrated detector L2.

The effect also occurs for a fraction of the iron nuclei which barely penetrate the L1 detectors. In this case, the affected events may be seen as the unusual clump of points near Z1=28 in Figure 3.6.

The above signature suggests a pulse height multiplication effect in the LET 35 um surface barrier detectors that is very similar to one observed earlier in the response of such detectors to fission fragments. The effect (discussed by Walter 1969) occurs for nuclei which deposit a large ionization charge density in the depleted silicon near the gold electrode. The large ionization charge density is thought to induce tunneling of additional carriers (electrons) from the electrode through the thin oxide layer which separates the electrode frm the depleted bulk silicon. The orientation of the LET 35 um detectors is consistent with this multiplication hypothesis: The gold electrodes face toward the L3 detector, such that the ionization charge density near a gold electrode is largest for nuclei which just barely penetrate the detector, as in (2) above.

To further stydy the problem, three detector PHA events with charge measurements Z1> 24 were re-analyzed. For each event the

L1 and L3 energy measurements (E{L1} and E{L3}) were used to calculate a new charge measurement Z' and obtain an estimate E'{L2} of the energy deposited in detector L2 by solving:

$$T\{L1\} = R(E\{L1\} + E'\{L2\} + E\{L3\},\ Z',\ M) - R(E'\{L2\} + E\{L3\},\ Z',\ M)$$
$$T\{L2\} = R(E'\{L2\} + E\{L3\},\ Z',\ M) = R(E\{L3\},\ Z',\ M)$$

taking $M = 2.132 * Z'$

R is the generalized range-energy function discussed in Section 3.4. T{L1} and T{L2} are the mean pathlengths for the L1 and L2 detectors respectively. The results are illustrated in Figure B.1, a plot of E{L2} (the measured L2 energy) versus E'{L2} (the L2 energy inferred from the L1 and L3 energy measurements). Normal events lie along the diagonal, while events with abnormally large L2 energy measurements lie above the diagonal. (Events below the diagonal may be due to L2 edge effects and other processes discussed in Section 3.5.2) The abnormal events occur predominantly at large values of E'{L2} which can only be obtained by nuclei which barely penetrate L2, consistent with observation (2) above. Figure B.2 shows two histograms of E{L2}/E'{L2} ; one histogram for events which barely penetrate L2 (E{L3} < 170 MeV) and one for the remaining events (E{L3} > 170 MeV). These histograms are summed over all the LETs used on both Voyagers and indicate that (1) about 15 percent of the events with E{L3} less than 170 MeV have L2 energy measurements which are abnormally large by an average of about 12 percent and (2) the L2 energy measurements are essentially normal for events with E{L3} greater than 170 MeV.

B.3.1 Three Parameter Analysis for Iron Nuclei

The results for iron nuclei presented in Table 4.2 (8.7-15.0 MeV/nucleon) are based on PHA events selected as follows:

(1) Normal iron events (i.e. those with normal L2 pulse height) were selected using the charge consistency requirement and charge boundaries discussed in Section 3.5, and were counted if the total energy measurement, E{L1}+E{L2}+E{L3}, was appropriate to the 8.7 - 15.0 MeV/nucleon interval.

(2) Iron PHA events having abnormally large L2 pulse heights were identified as those events with charge measurements near (Z1=26, Z2=28). (Specifically, the requirement was (Z1+Z2)/2 > 25 and (Z1-Z2) < -0.85.) For each of the PHA events the L2 energy measurement was divided by 1.125 (the mean shift of the abnormal L2 energy measurements; see Figure B.2) to obtain a corrected value E*{L2}. Then the event was counted if E{L1}+E*{L2}+E{L3} was within the total energy interval corresponding to 8.7 - 15.0 MeV/nucleon.

PHA events with abnormal L2 pulse heights constitute about 15 percent of the iron nuclei counts presented in Table 4.2. Any additional systematic error (beyond that discussed in Section 4.4.1) in the iron nuclei counts due to the abnormal L2 pulse heights should be small. For example, if no corrections at all are applied to the abnormal L2 energy measurements (as was the case for the iron abundances reported earlier in Cook et. al. 1979 and Cook, Stone

and Vogt 1980), the resulting iron abundance measurements differ from those of Table 4.2 by less than 5 percent.

B.3.2 Two Parameter Analysis for Iron Nuclei

In the two parameter analysis of iron (for the fluence measurements of Tables 4.4 through 4.11) the multiplication effect in the L1 detectors was taken into account as follows:

(1) Iron PHA events with normal L1 pulse heights were identified as those events with charge measurement Z1 in the range 24.8 to 27.2 and were binned according to energy/nucleon as described in Section 3.4.

(2) PHA events with charge Z1 in the range 27.2 to 32.0 and L2+L3 energy measurements of less than 170 MeV are primarily due to iron nuclei with abnormally large L1 pulse heights, rather than nickel or other nuclei. Therefore, the L1 energy measurements of these events were divided by 1.125 before energy/nucleon binning. The remaining events with Z1 in the range 27.2 to 32.0 (i.e. those with E{L2}+E{L3} > 170 MeV) are mainly nickel nuclei an were included with no L1 energy adjustment. All PHA events were sorted into energy/nucleon binns as if they were due to iron nuclei, exactly as in (1) above.

In the two parameter iron analysis, no special treatment was applied to account for multiplication effects in the L2 detectors. They do not significantly affect the Z1 charge measurement and at most shift a small fraction (about 5 percent) of the PHA events which should fall in th 7.8-8.7 MeV/nucleon interval into the 8.7 - 10.6 MeV/nucleon interval.

The inclusion of nickel and other nuclei ($27 <= Z <= 32$) increases the fluence measurements over measurements of pure iron by roughly the combined abundance of these elements relative to iron, or about 10 percent. However, the inclusion of these nuclei probably has only a negligible effect on the spectral index(gamma, see Section 4.5), since the energy spectra of the various elements of the iron group are likely to be similar. (Spectral index variations among the elements appear to be roughly ordered by nuclear charge Z, such that, in a given flare event, neighboring elements have similar spectral indices; see Section 5.2. Further, the nickel to iron ratio {8.7 -15 MeV/nucleon, Table 4.2} is nearly constant from flare to flare.)

The multiplication effect in the L1 detectors is potentially an additional source of systematic error (beyond those discussed in Section 4.5) in the iron fluence measurements of Tables 4.4 through 4.11 and the iron spectral index measurements of Tabl 4.12. Upper limits to these possible additional errors were obtained by re-computing the fluences and spectral indices without the L1 energy corrections discussed in (2) above. The changes in the iron fluence measurements were typically less than 10 percent for energy bins in the range 5.0-8.7 MeV/nucleon, and wer zero for the other higher energy bins. The iron spectral indices changed by less than 5 percent. Since the actual systematic error induced in the iron spectral indices is probably much less than 5 percent (and therefore is small compared to statistical error and the possible systematic error from other sources discussed in Section 4.5) this error is negligible.

HH Breneman Thesis. Flare analysis treated differently from interplanetary data.

Appendix G Instrumental Anomalies and Other Problems

The analysis of data form the Voyager CRS LET and HET telescopes was complicated by several instrumental problems. These are described in detail elsewhere (Breneman 1984); they are summarized here.

G.1. Pulse Height 'Multiplicaton' Effect

This effect has been observed many times in numerous surface-barrier detectors, both in flight and in the laboratory (Cook 1981, Breneman 1982). Particles passing completely through a detector sometimes yield pulse heights that are anomalously high By about 10 - 30 %). It occurs most often for particles with high dI/dx in the detector in question, and therefore at a given initial energy, the errect occurs more often for elements higher on the charge scale; in the data it is most prominent for Fe. On a delta E versus E' plot, the effect appears as a more or less diffuse 'track' above and roughly parallel to the nominal track for the element, since delta E is anomalously high for the affected particles (Fig. G.1). A charge determination of such an event will of course be high, generally by ~2-3 charge units at Fe. Since the effect is strongly dependent on dE/dx, it is usually evident only in the delta E detector immediately before the E' detector. When z is calculated for 3-parameter events involving such anomalous pulse heights, Z2 is more strongly affected than Z1, since the anomalous pulse height has the role of delta E for Z2, while for Z1 the same detector PHA usually makes only a modest contribution to E' with delta E normal. On a Z1 versus Z2 plot (e.e., Fig. 3.1), the effect takes the form of a cluster fo events to the right of, and slightly above, the main cluster along the diagonal. All of the Voyager LETs show the effect for Fe; although its rate of occurrence varies somewhat between the different telescopes, it is generally in the range of ~5 - 10 % of all the 3-parameter Fe SEP events in a given telescope. The fraction of 2-parameter events affected is larger, since the E' detector is thinner and therefore a larger fraction of the data has high dE/dx in the delta E detector. At least one LET (Voyager 1 LET A) shows evidence for the effect at charges as low as 20.

In the HETs the problem is worse in several respects. Its rate of occurrence at Fe, as a percentage of the total Fe event ample, is generally much larger than in the LETs (~40 % for Voayger 1 HET 2); it is clearly seen for elements as low on the charge scale as Mg in some telescopes (Voyager 1 HET 2 and Voyager 2 HET 2); and for 3-parameter events it can sometimes be seen occurring in either (or both) delta E detectors, rather than just the last one, resulting in several displaced clusters of events in those telescopes (Voyager 1 HET 1 and Voayger 2 HET 2).

Two actions were necessary to deal with this problem. For

abundant elements affected by the problem, mainly Fe and Ni, the 3-parameter charge consistency requirement was made lenient enough to include the particles affected by pulse height multiplication. The rate of occurrence in LET for elements lower than Fe was negligible compared to other sources of uncertainty in the abundance determination, and no correction was made for these elements. Based on the observed rates in some HET telescopes for the abundant elements (e.e., Fig. G.2 for Voayger 1 HET 2), the rate of occurrence in these thelscopes for elements in the Z = 17-25 charge range was significant even though limited statistics make it less apparent and less quantifiable. However, HET data were not used for these elements for the reasons given in Section 3.3.

In addition, the energy loss in the delta E detector had to be corrected in an approximate way for affected events, so that the total incident energy, which is required for constructing energy spectra, would be accurate.

For 2-parameter events, there is no second independent determination fo Z to permit unambiguous separation of normal and abnormal events. This is not a serious problem for abundant elements, since the only abundant element significantly affected is Fe, which has no other elements of comparable abundance near it on the charge scale with which it could be confused. For rare elements the situation would be more serious, but as noted in Section 3.3, 2-parameter data were not used for rare element abundances due to excessive background contamination from other sources.

G.2. LET Telescope ID Tag Bit Errors at High Counting Rates

For each Block I or Block II LET event, there is a single tag bit which specifies from whih LET telescope in that Block the event originated. A near coincidence in the triggering of LETs A and B, as is possible during periods of very high count rates, can result in the bit being set for a LET A event, causing that event to be read out as a LET B event (similarly for C and D). Since the bit is ordinarily set only for LET B events and is otherwise not set, LET A events can be misidentified as LET B events but never the reverse.

The telescope identification bit is used in all subsequent data analysis to determine the appropriate detector thicknessess and gains to use in calculating energy losses in the detectors and, ultimately, the charge of the particle. If the telescope identification is erroneous, incorrect thick= nesses and gains are used in the calculations, resulting in incorrect determinations of Z. The magnitude and sign of the discrepancy in Z depends only on the (coincidental) relationship between the thicknesses of the detectors in the paired telescopes, and, to a lesser degree, differences in the energy calibrations fo the respective detectors.

On a Z1 versus Z2 plot of 3-parameter Voyager data, this effect has the appearance of small clusters of events displaced slightly from the main clusters along the diagonal for all the more abundant elements. It appears only in

plots of the B and D telescopes, sine it is events with these identifications which contain some misidentified particles. In the Voyager flight data the effect is noticeable only during flare period 7, for which the peak LET B singles rate is ~ 5 * 10**3 /sec, the highest seen during the Voayger mission through August 1984. Its rate of occurrence is about 3 % at this peak rate, an average of about 1 % for flare period 7 as a whole, and is the same for all elements for which statistics permit a measurement. On delta E versus E' plots of both 2- and 3-parameter data, these effects have the appearance of 'ghost' tracks falling between or partially overlapping the real tracks of nearby elements (Fig. G.3).

Later laboratory work using the backup GRS and pulse generators (Martin 1983) was able to reproduce the effect with greatly improved statistics, and verified the magnitude of the time constant (~6 us) implied by the flight data while extending coverage to event rates more than an order of magnitude above the highest seen in the flight data.

The impact of this problm on the data analysis is relatively minor. For 3-parameter data, the previously chosen charge-consistency requirement is restrictive enough to easily exclude the misidentified events; the amount of data lost is an insignificant 0.2% of the total, and the remaining data set is as 'clean' as that from the other telescopes. The problem is more serious for the 2-parameter data, since there is no second determination of Z to permit separation of the normal and abnormal events; it is an unremovable source of background in the data. For abundant elements this is unimportant, since the error introduced by this background is on the order of 1 % or less. But the problem would be serious for rare elements in cases where the 'ghost' trakc of an abundant element overlaps the true location fo a rare element, since even 1 % of an abundant element could seriously contaminate a much rarer element. However, as noted previously, the 2-parameter LET data are not useful in obtaining rare element abundances on account of other background contributions.

G.3. LET L1 Detector Jupiter Encounter Radiation Damage and Post-Encounter Annealing

As a result of their exposure to intense charged particle fluxes in the inner Jovian magnetosphere during the 1979 Jupiter encounters, the L1 detectors of the LETs experienced radiation damage which can be modeled as a reduction in the 'effective thickness' of the detectors. It is thought to be due to the implantation of energetic oxygen and sulfur ions known to be present in the inner Jovain magnetosphere (Gehrels 1982). Although all LETs on both spacecraft were affected to some degree, the Voayger 1 LETs were affected much worse than those on Voyager 2, since the former spacecraft passed closer to Jupiter and experienced a more intense radiation environment. On each spacecraft, LET C was by far the most seriously affected; this telescope was sparially oriented so as to receive the most intense radiation exposure during the Jupiter encounters. (LET B on Voyager 2 experienced unrelated types

of radiation damage during the Jovian encounter and has returned no data since tha encounter.) The front detectors of the HETs, being much thicker than those of the LETs and protected by a thiker window, showed no detectable effective thichness reduction.

The impact of the radiation damage on the post-Jupiter data is apparent as a shift in the location fo the element tracks on a delta E versus E' plot of data from flares 16 and 17, the first large post-Jupiter flares, relative to their location in plots of pre-Jupiter flares. Similarly, Z1 versus Z2 plots of flares 16 and 17 show Z values shifted from their proper values when Z is calculated using the detector thicknesses measured before launch, which served adequately for all pre-Jupiter flares. The change in effective thickness appears to be somewhat dependent on Z, with the magnitude of the reduction increasing with Z for any given detector. Furthermore, with the passage of time the radiation damage seems to gradually undergo a partial reversal. This 'annealing' effect is evident in data from the later large flares, 20 and 24, which show less shift in Z than do the flares immediately following Jupiter encounter.

In the analysis of post-Jupiter data, this problem was dealt with by adjusting the L1 detector thicknesses used in the calculation of Z so as to make the calculated charges fall in the proper places on the charge scale. Flares 16 and 17 were used to define the required shift for the more abundant elements; a linear or weakly quadratic function of Z was fit to these to define the Z dependence for all Z. Data from flare periods 20 and 24 were used in conjunction with the flare 16/17 data to mathematically characterize the time-dependence of the annealing effect, by fitting to a decaying-exponential function of time. This procedure, repeated for each LET, defined the L1 thickness to be used in analyzing any given post-Jupiter event. The adjustment of the L1 thickness was then incorporated into the iterative cycle for calculating Z. The radiation damage did not have a noiceable effect on the inherent charge resolution of the telescopes, so with the above modifications the post-Jupiter flare data could be treated the same way as the pre-Jupiter data.

Table G.1 lists the adjustment made to the thickness for each L1 detector cor carbon and iron at two different times during the post-Jupiter phase. The actual expression for the thickness L(Z,t) of each L1 detector was given by

$$L(Z,t) = L0 - \text{deltaL0}(Z) + K \exp(\text{delta t} / 562.56)$$

where K is a constant, L0 is the pre-Jupiter thickness, delta t is the time since the Jupiter encounter in days, and deltaL0(z) is the linear or quadratic function of Z that closely fits the required thickness changes for the first post-Jupiter flares.

G.4. Voyager 2 LET C Temporary Gain Shift

During the time period 1978 APR 3 - June 9, the L1 detector of LET C on Voayger 2 experienced, for unknown reasons, a

temporary gain shift (~ 47 % decrease) and an associated excessively high L1 count rate (~ 9* 10**3 /sec). The gain shift and excessive count rate set in abruptly, remained nearly constant until about May 29, and then gradually reverted to their former levels; a very slight decline during the central phase was consistent with the decrease in the intensity of sunlight during the smae time period and suggests the possibility of a light leak in the telescope's aluminum window.

The effect on the data was to shift the locations of the element tracks on a delta E versus E' plot, and yield shifted charge estimates when nominal gain factors were used in the analysis. The only flares occurring duting this time period were the three large events of flare period 7. Since the gain was constant at the shifted value during these flares, the data could be analyzed by generating the appropriate gain factors by fitting the oxygen flight data from flare period 7 in the manner described in Appendix A. The resulting values are included in Table A.1.

This anomaly was previously noted (Cook 1981), and the telescope was rejected for analysis because of the problem. However, since the energy calibration used in the analysis is easily adjusted to compensate for the problem, since the charge resolution and background of the telescope do not seem to be affected by the problem and since the three 7 flares include a major fraction of all SEP data, it was decided to inlude Voayger 2 LET C in the analysis with the special treatment described above.

G.5 CRS Instrument Configuration Changes

At certain times during the Voayger mission, the configuation of the CRS instruments was changed in ways that influence data analysis. At the beginning of each flight the LETs were configured to require triggering of the L3 detector for pulse height analysis; that is, only 3-parameter events were analyzed. About 12 days after launch the L3 coincidence requirement was removed, permitting both 2- and 3-parameter events to be analyzed. For Voyager 2 this occurred before the first flares were seen, but on Voyager 1 flares 1a and 1b occurred before the configuration was changed, so no 2-parameter events were obtained from these flares. A similar situation occurred on 17 Jun 1978 when Voyager 1 LET C was switched back to requiring L3 coincidence. Thus for all flares from 8 onward there are no 2-parameter events from this telescope. These situations required changes in the weightings of 2-parameter relative to 3-parameter events for the affected spacecraft and flares. There could still be a residual abundance bias in flares 1a dna 1b if the particle composition was energy-dependent and if the two spacecraft saw particles with different spectra, but the possibility of a bias comparable to the statistical uncertainty in the abundances is very unlikely.

Another important configuration change is the HET gain state. Normally the instrument cycles between high and low gain

modes, but after Jupiter encounter HET 1 on Voyager 2 was switched to a high-gain-only mode, so no post-Jupiter SEP heavy ion data were obtained from this telescope. This required changes in the partile wwighting factors of HET relative to LET for Voyager 2 for all post-Jupiter flares.

The event weighting factors tabulated in Table 3.8 include the effects of all instrument configuration changes.

G.6. Voyager 1 Block I PHA Problem

On 1982 Feb 8, the Voayger 1 CRS experienced a failure affecting the readout of PHA information from the Block I telescopes (LETs A and B and HET 1). The result of the failure is that in place of PHA2, the instrument reads out whichever of the three PHAs has the largest numerical value. If PHA2 happens to be numerically the largest pulse height, as is true over some energy ranges, the event is read out normally; otherwise some information si lost. The effect of this problem is that some of the 2-parameter events are lost completely, and that some of the 3-parameter events are degraded to 2-parameter events.

The effect of this problem on the data analysis was minimal because it occurred very late in the time span included in the SEP data set, and thus affected only two relatively small flares. The problem was dealt with by simply discarding the data on these flares from the three telescopes affected.

END OF THESIS INFORMATION ----------

Summary of Voyager-1 LET L1 thickness and delta Z correction from Dr. Cummings:

LET L1 Thickness before VOLUME 94465

= 37.91 um LET A
30.91 um LET B
37.07 um LET C
35.45 um LET D
um = micrometers

LET L1 Thickness after VOLUME 94465

= 37.09 um + 0.82 {1 - exp{-(boi-94465)/943693} } LET A
27.97 um + 0.94 {1 - exp{-(boi-94465)/943693} } LET B
30.81 um + 6.26 {1 - exp{-(boi-94465)/943693} } LET C
34.68 um + 0.77 {1 - exp{-(boi-94465)/943693} } LET D
um = micrometers

Z1 is computed from L1 vs L2+L3 energies
After VOLUME 94465 Z1 is corrected as follows if Z1 > 9,
rho{123} = (E{L1}+E{L2}+E{L3}) / 2Z1 < 25

Z1' = Z1 + delta Z where

delta Z{A} = (Z1/26)**2 x (1.0461- 0.0418(rho{123})) x
{1 - exp{-(boi-94465)/943693} }

```
  delta Z{B} = (Z1/26)**2 x (0.9254- 0.0370(rho{123})) x
                            {1 - exp{-(boi-94465)/943693} }

  delta Z{C} = (Z1/26)**2 x (1.5190- 0.0608(rho{123})) x
                            {1 - exp{-(boi-94465)/943693} }

  delta Z{D} = (Z1/26)**2 x (0.8730- 0.0349(rho{123})) x
                            {1 - exp{-(boi-94465)/943693} }
```

Summary of Voyager-2 LET C L1 thickness and delta Z correction (post-Jupiter) from Dr. Cummings:

```
  LET C L1 Thickness before VOLUME 93985
            = 35.33 um    LET C
                          um = micrometers

  LET C L1 Thickness after  VOLUME 93985
            = 32.43 um + 2.90 {1 - exp{-(boi-93985)/943693} }
                          um = micrometers

  Z1 is computed from L1 vs L2+L3 energies
  After VOLUME 93985 Z1 is corrected as follows if Z1 > 9,
               rho{123} = (E{L1}+E{L2}+E{L3}) / 2Z1   <   25 ,
               and if LET = C or D :

  Z1'  =  Z1 + delta Z  where

  delta Z{C} = (Z1/26)**2 x (1.8530- 0.0741(rho{123})) x
                            {1 - exp{-(boi-93985)/943693} }

  delta Z{D} = (Z1/26)**2 x (0.6970- 0.0279(rho{123})) x
                            {1 - exp{-(boi-93985)/943693} }
```

DATA_PROCESSING_OVERVIEW: Four generic types of data are sent back by the cosmic ray telescopes: rates data, pulse height data, internal calibration data and engineering housekeeping data. All are preserved in the reduction steps described below.

A time-ordered dataset containing fifteen minute data blocks (VOLUMEs) of PHA and RATE data is created from the experimenter data records. The data are decompressed and reorganized while preserving the time order. Each VOLUME contains summarized counts and accumulation times for RATES. In addition, the PHA data is sorted and organized by event types. Time tags of individual particles are lost in this process. This database is called the ENCYCLOPEDIA Database.

Using the instrument response matrices and the ENCY database, rates and particle fluxes averaged over multiples of fifteen minutes can be derived. The desired count rates and fluxes are computed on demand, and the NSSDC data is produced in this manner. We have submitted encounter data at 15 minute resolution and the rest of the data at 6 hour time resolution. The interplanetary dataset submitted to NSSDC may be periodically updated, and the new submission will supercede the previous data.

ENCY database volumes for Voyager-1 and Voyager-2 are approximately 5 Gbytes each. All permanent databases reside on magnetic tape volumes in the library at the NCCS IBM 9021.

This data set is not intended to be used as an encounter data set.

LIT_REFERENCES:

INSTRUMENTATION

D.E.Stillwell, W.D.Davis, R.M.Joyce, F.B.McDonald, J.H.Trainor, W.E.Althouse, A.C.Cummings, T.L.Garrard, E.C.Stone, and R.E.Vogt, "The Voyager Cosmic Ray Instrument", ISEE Transactions on Nuclear Science, Vol. 26, 1979, pp. 513

SCIENTIFIC PAPERS

See the file VOYAGER-REFERENCES in the data directory

VOL_TIME_COVERAGE: 1977-08-24 to 1993-12-31

FILE_NAMING_CONVENTION: CRS files are named according to the start time of the data contained in the file as follows: V2xx.NSSDC . Here the xx stands for the two digits of the year of the data contained in the file. For the 1979 major section split V279A and V279B are used. Name 1982 analagously. The 1978 data V278P start from February 19 for this release.

FILE_TIME_COVERAGE:
Data appear as one file for each year from 1977 - 1993 with the exceptions noted immediately above.

V277.NSSDC 1977 launch - 78/01/01 00:00:00

Other similarly named files contain each year's data starting from January 1.

/* EOF */
/* list of data quantities in order on the files follows */

SUBM_NAME: Dr. Nand Lal
SUBM_ADDR: Goddard Space Flight Center
Code 935
Greenbelt, MD 20771

Electronic mail: nand@voyager.gsfc.nasa.gov
LHEAVX::LAL
SUBM_DATE: 1994-10-07
TITLE: Format for Voyager-2 CRS Cruise Data Archive Data Set
DESCR: Format description of the Voyager-2 Cosmic Ray Subsystem cruise phase energetic particle data measurements archive data set, August 24, 1977

through 1993.
REL_DATE: 1994-10-07

RECORD_FIELD_MNEMONICS: See above in the DATA_SET_PARAMETERS for basic description of quantities.

For section 1 time period:

```
* VOYAGER-2 NSSDC SUBMISSION NUMBER 1 BINCARDS;  SET 1 data quantities
*
*     DIVIDE INTO THREE MAIN SETS OF CARDS,
*     - SET 1 WILL BE AUTOGAIN MODE, VERY SIMILAR TO V1FBINS
*       LAUNCH - JUPITER  USE ~6/29/79
                        TIME,
                        HELIUMFLUX1,
                        HELIUMFLUX2,
                        HELIUMFLUX3,
                        HELIUMFLUX4,
                        HELIUMFLUX5,
                        HELIUMFLUX6,
                        HELIUMFLUX7,
                        HELIUMFLUX8,
                        PROTONFLUX1,
                        PROTONFLUX2,
                        PROTONFLUX3,
                        PROTONFLUX4,
                        PROTONFLUX5,
                        HELIUMFLUX9,
                        HELIUMFLUX10,
                        HELIUMFLUX11,
                        HELIUMFLUX12,
                        HELIUMFLUX13,
                        HELIUMFLUX14,
                        HELIUMFLUX15,
                        HELIUMFLUX16,
                        PROTONFLUX6,
                        PROTONFLUX7,
                        PROTONFLUX8,
                        PROTONFLUX9,
                        PROTONFLUX10,
                        PROTONFLUX11,
                        PROTONFLUX12,
                        PROTONFLUX13,
                        PROTONFLUX14,
                        PROTONFLUX15,
                        PROTONFLUX16,
                        PROTONFLUX17,
                        PROTONFLUX18,
                        HELIUMFLUX17,
                        HELIUMFLUX18,
                        HELIUMFLUX19,
                        HELIUMFLUX20,
                        HELIUMFLUX21,
                        HELIUMFLUX22,
                        HELIUMFLUX23,
                        HELIUMFLUX24,
```

BRIAS

BRIASZ3 .
BRIBSE .
BRIBSP .
BRIBSZ2 .
BRIPENL .
BRIPENH .
BRIPGL .
BRIPGH .
BRIBS4E .
BRIBS4P .
BRIBS4 .
BRIBS4Z2 .
BRIBS2E .
BRIBS2P .
BRIBS2 .
BRIBS2Z2 .
BRIBS3E .
BRIBS3P .
BRIBS3 .
BRIBS3Z2 .
BRISA1 .
BRISA2 .
BRIG1 .
BRIISA1 .
BRIISA2 .
BRIIG1 .
BRIIAS .
BRIIASZ3 .
BRIIBSE .
BRIIBSP .
BRIIBSZ2 .
BRIIPENL .
BRIIPENH .
BRIIPGL .
BRIIPGH .
BRIIBS4E .
BRIIBS4P .
BRIIBS4 .
BRIIBS4Z2 .
BRIIBS2E .
BRIIBS2P .
BRIIBS2 .
BRIIBS2Z2 .
BRIIBS3E .
BRIIBS3P .
BRIIBS3 .
BRIIBS3Z2 .
BRIA1H .
BRIA2H .
BRIB1H .
BRIB2H .
BRIC1H .
BRIC2H .
BRIC3H .
BRIC4H .
BRISBH .
BRIA1L .
BRIA2L .
BRIB1L .

BRIB2L .
BRIC1L .
BRIC2L .
BRIC3L .
BRIC4L .
BRISBL .
BRIIA1H .
BRIIA2H .
BRIIB1H .
BRIIB2H .
BRIIC1H .
BRIIC2H .
BRIIC3H .
BRIIC4H .
BRIISBH .
BRIIA1L .
BRIIA2L .
BRIIB1L .
BRIIB2L .
BRIIC1L .
BRIIC2L .
BRIIC3L .
BRIIC4L .
BRIISBL .
BRLA1 .
BRLB1 .
BRLC1 .
BRLD1 .
BRLA2 .
BRLB2 .
BRLC2 .
BRLD2 .
BRLA3 .
BRLB3 .
BRLC3 .
BRLD3 .
BRLA4 .
BRLB4 .
BRLC4 .
BRLD4 .
BRSLA .
BRSLB .
BRSLC .
BRSLD .
BRLATRP .
BRLBTRP .
BRLCTRP .
BRLDTRP .
BRD1L .
BRD2L .
BRD3L .
BRD4L .
BRD5L .
BRD6L .
BRD7L .
BRD8L .
BRGA+GB .
BRD1H .
BRD2H .

```
BRD3H           .
BRD4H           .
BRD5H           .
BRD6H           .
BRD7H           .
*  MAJOR STATUS CHANGE CONFIGURATIONS IN CRUISE AFFECT THESE
BRLC            .                                                       X
                                                                        X

  L1.L2.L3.^SL.^L4
BRLC            .                                                       X
                                                                        X

  L1.L2.^SL.^L4
BRLCZ3          .                                                       X
                                                                        X

  L1.L2.L3.SL.^L4
BRLCZ3          .                                                       X
                                                                        X

  L1.L2.SL.^L4
BRLD            .                                                       X
                                                                        X

  L1.L2.L3.^SL.^L4
BRLD            .                                                       X
                                                                        X

  L1.L2.^SL.^L4
BRLDZ3          .                                                       X
                                                                        X

  L1.L2.L3.SL.^L4
BRLDZ3          .                                                       X
                                                                        X

  L1.L2.SL.^L4
BRLA            .                                                       X
                                                                        X

  L1.L2.L3.^SL.^L4
BRLA            .                                                       X
                                                                        X

  L1.L2.^SL.^L4
BRLAZ3          .                                                       X
                                                                        X

  L1.L2.L3.SL.^L4
BRLAZ3          .                                                       X
                                                                        X

  L1.L2.SL.^L4
BRLB            .                                                       X
                                                                        X

  L1.L2.L3.^SL.^L4
BRLB            .                                                       X
                                                                        X

  L1.L2.^SL.^L4
BRLBZ3          .                                                       X
                                                                        X

  L1.L2.L3.SL.^L4
BRLBZ3          .                                                       X
                                                                        X

  L1.L2.SL.^L4
BRTAN           .                                                       X
                                                                        X

  W1.W2.D3.^D8.^GA.^GB
BRTAN           .                                                       X
                                                                        X
```

```
  W1.W2.^D8.^GA.^GB
BRTLO        .
BRTLO        .                                                          X
                                                                        X
  W1.W2.D5.^D6.^GA.^GB.^UT
BRTHI        .
BRTHI        .                                                          X
                                                                        X
  W1.W2.D7.^D8.^GA.^GB.^UT


For section 2 time period:

* VOYAGER-2 NSSDC SUBMISSION NUMBER 1 BINCARDS   SET 2 CARDS
* 8/22/79 - 4/22/82
*     - SET 2 HAS HET I GAIN SET HIGH WITH CYCLING OF THAT AND OTHER
*        8/22/79 19:30 - 10/24/97 CYCLING OF SOME WORDS
*       10/24/79 17:30 - 10/20/81 22:45  STABLE
*       10/20/81 22:45 -  4/21/82 17:30  CYCLINGS VARIOUS
                        TIME,
                        HELIUMFLUX1,
                        HELIUMFLUX2,
                        HELIUMFLUX5,
                        HELIUMFLUX6,
                        HELIUMFLUX8,
                        PROTONFLUX1,
                        PROTONFLUX2,
                        PROTONFLUX3,
                        PROTONFLUX4,
                        PROTONFLUX5,
                        HELIUMFLUX11,
                        HELIUMFLUX12,
                        HELIUMFLUX15,
                        PROTONFLUX11,
                        PROTONFLUX13,
                        PROTONFLUX14,
                        PROTONFLUX15,
                        PROTONFLUX17,
                        PROTONFLUX18,
                        HELIUMFLUX17,
                        HELIUMFLUX19,
                        HELIUMFLUX20,
                        HELIUMFLUX21,
                        HELIUMFLUX23,
                        HELIUMFLUX24,
*  LOW GAIN OUT        *R in colums 1,2 indicates not present
BRIAS        .
*RIASZ3      .
BRIBSE       .
BRIBSP       .
*RIBSZ2      .
*RIPENL      .
BRIPENH      .
*RIPGL       .
BRIPGH       .
BRIBS4E      .
BRIBS4P      .
*RIBS4       .
*RIBS4Z2     .
```

```
BRIBS2E      .
BRIBS2P      .
*RIBS2       .
*RIBS2Z2     .
BRIBS3E      .
BRIBS3P      .
*RIBS3       .
*RIBS3Z2     .
BRISA1       .
BRISA2       .
BRIG1        .
*  II  LOW GAIN ONLY
BRIISA1      .
BRIISA2      .
BRIIG1       .
*RIIAS       .
BRIIASZ3     .
*RIIBSE      .
*RIIBSP      .
BRIIBSZ2     .
BRIIPENL     .
*RIIPENH     .
BRIIPGL      .
*RIIPGH      .
*RIIBS4E     .
*RIIBS4P     .
BRIIBS4      .
BRIIBS4Z2    .
*RIIBS2E     .
*RIIBS2P     .
BRIIBS2      .
BRIIBS2Z2    .
*RIIBS3E     .
*RIIBS3P     .
BRIIBS3      .
BRIIBS3Z2    .
*  I HIGH GAIN ONLY    II LOW GAIN ONLY
BRIA1H       .
BRIA2H       .
BRIB1H       .
BRIB2H       .
BRIC1H       .
BRIC2H       .
BRIC3H       .
BRIC4H       .
BRISBH       .
*RIA1L       .
*RIA2L       .
*RIB1L       .
*RIB2L       .
*RIC1L       .
*RIC2L       .
*RIC3L       .
*RIC4L       .
*RISBL       .
*RIIA1H      .
*RIIA2H      .
*RIIB1H      .
*RIIB2H      .
```

```
*RIIC1H      .
*RIIC2H      .
*RIIC3H      .
*RIIC4H      .
*RIISBH      .
BRIIA1L      .
BRIIA2L      .
BRIIB1L      .
BRIIB2L      .
BRIIC1L      .
BRIIC2L      .
BRIIC3L      .
BRIIC4L      .
BRIISBL      .
BRLA1        .
*RLB1        .
BRLC1        .
BRLD1        .
BRLA2        .
BRLB2        .
BRLC2        .
BRLD2        .
BRLA3        .
BRLB3        .
BRLC3        .
BRLD3        .
BRLA4        .
BRLB4        .
BRLC4        .
BRLD4        .
BRSLA        .
BRSLB        .
BRSLC        .
BRSLD        .
BRLATRP      .
BRLBTRP      .
BRLCTRP      .
BRLDTRP      .
BRD1L        .
BRD2L        .
BRD3L        .
BRD4L        .
BRD5L        .
BRD6L        .
BRD7L        .
BRD8L        .
BRGA+GB      .
BRD1H        .
BRD2H        .
BRD3H        .
BRD4H        .
BRD5H        .
BRD6H        .
BRD7H        .
*  MAJOR STATUS CHANGE CONFIGURATIONS IN CRUISE AFFECT THESE
BRLC         .                                                    X
                                                                  X
  L1.L2.L3.^SL.^L4
BRLC         .                                                    X
```

```
                                                                    X
  L1.L2.^SL.^L4
BRLCZ3        .                                                     X
                                                                    X
  L1.L2.L3.SL.^L4
BRLCZ3        .                                                     X
                                                                    X
  L1.L2.SL.^L4
BRLD          .                                                     X
                                                                    X
  L1.L2.L3.^SL.^L4
BRLD          .                                                     X
                                                                    X
  L1.L2.^SL.^L4
BRLDZ3        .                                                     X
                                                                    X
  L1.L2.L3.SL.^L4
BRLDZ3        .                                                     X
                                                                    X
  L1.L2.SL.^L4
BRLA          .                                                     X
                                                                    X
  L1.L2.L3.^SL.^L4
BRLA          .                                                     X
                                                                    X
  L1.L2.^SL.^L4
BRLAZ3        .                                                     X
                                                                    X
  L1.L2.L3.SL.^L4
BRLAZ3        .                                                     X
                                                                    X
  L1.L2.SL.^L4
BRLB          .                                                     X
                                                                    X
  L1.L2.L3.^SL.^L4
BRLB          .                                                     X
                                                                    X
  L1.L2.^SL.^L4
BRLBZ3        .                                                     X
                                                                    X
  L1.L2.L3.SL.^L4
BRLBZ3        .                                                     X
                                                                    X
  L1.L2.SL.^L4
BRTAN         .                                                     X
                                                                    X
  W1.W2.D3.^D8.^GA.^GB
BRTAN         .                                                     X
                                                                    X
  W1.W2.^D8.^GA.^GB
BRTLO         .
BRTLO         .                                                     X
                                                                    X
  W1.W2.D5.^D6.^GA.^GB.^UT
BRTHI         .
BRTHI         .                                                     X
                                                                    X
  W1.W2.D7.^D8.^GA.^GB.^UT
```

For section 3 time period:

```
* VOYAGER-2 NSSDC SUBMISSION NUMBER 1 BINCARDS   SET 3 CARDS
* tape data START AT 4/21/82 00:00
*      - SET 3 HAS HET I GAIN SET HIGH AND OTHER STABLE
*        4/21/82 17:30 - EOD  EXCEPT FOR TAN TO NOMINAL AT 3/12/85
                         TIME,
                         HELIUMFLUX1,
                         HELIUMFLUX2,
                         HELIUMFLUX5,
                         HELIUMFLUX6,
                         HELIUMFLUX8,
                         PROTONFLUX1,
                         PROTONFLUX2,
                         PROTONFLUX3,
                         PROTONFLUX4,
                         PROTONFLUX5,
                         HELIUMFLUX11,
                         HELIUMFLUX12,
                         HELIUMFLUX15,
                         PROTONFLUX11,
                         PROTONFLUX13,
                         PROTONFLUX14,
                         PROTONFLUX15,
                         PROTONFLUX17,
                         PROTONFLUX18,
                         HELIUMFLUX17,
                         HELIUMFLUX19,
                         HELIUMFLUX20,
                         HELIUMFLUX21,
                         HELIUMFLUX23,
                         HELIUMFLUX24,
*  LOW GAIN OUT      *R in cols 1,2 indicates not present
BRIAS         .
*RIASZ3        .
BRIBSE        .
BRIBSP        .
*RIBSZ2        .
*RIPENL        .
BRIPENH       .
*RIPGL         .
BRIPGH        .
BRIBS4E       .
BRIBS4P       .
*RIBS4         .
*RIBS4Z2       .
BRIBS2E       .
BRIBS2P       .
*RIBS2         .
*RIBS2Z2       .
BRIBS3E       .
BRIBS3P       .
*RIBS3         .
*RIBS3Z2       .
*  THESE 3 OUT BECAUSE OF G1 BIT STUCK PROBLEM  AND THEY ARE LOW GAIN
*RISA1         .
*RISA2         .
*RIG1          .
```

```
*  II  LOW GAIN ONLY
BRIISA1      .
BRIISA2      .
BRIIG1       .
*RIIAS       .
BRIIASZ3     .
*RIIBSE      .
*RIIBSP      .
BRIIBSZ2     .
BRIIPENL     .
*RIIPENH     .
BRIIPGL      .
*RIIPGH      .
*RIIBS4E     .
*RIIBS4P     .
BRIIBS4      .
BRIIBS4Z2    .
*RIIBS2E     .
*RIIBS2P     .
BRIIBS2      .
BRIIBS2Z2    .
*RIIBS3E     .
*RIIBS3P     .
BRIIBS3      .
BRIIBS3Z2    .
*  I HIGH GAIN ONLY    II LOW GAIN ONLY
BRIA1H       .
BRIA2H       .
BRIB1H       .
BRIB2H       .
BRIC1H       .
BRIC2H       .
BRIC3H       .
BRIC4H       .
BRISBH       .
*RIA1L       .
*RIA2L       .
*RIB1L       .
*RIB2L       .
*RIC1L       .
*RIC2L       .
*RIC3L       .
*RIC4L       .
*RISBL       .
*RIIA1H      .
*RIIA2H      .
*RIIB1H      .
*RIIB2H      .
*RIIC1H      .
*RIIC2H      .
*RIIC3H      .
*RIIC4H      .
*RIISBH      .
BRIIA1L      .
BRIIA2L      .
BRIIB1L      .
BRIIB2L      .
BRIIC1L      .
BRIIC2L      .
```

```
BRIIC3L         .
BRIIC4L         .
BRIISBL         .
BRLA1           .
*RLB1           .
BRLC1           .
BRLD1           .
BRLA2           .
BRLB2           .
BRLC2           .
BRLD2           .
BRLA3           .
BRLB3           .
BRLC3           .
BRLD3           .
BRLA4           .
BRLB4           .
BRLC4           .
BRLD4           .
BRSLA           .
BRSLB           .
BRSLC           .
BRSLD           .
BRLATRP         .
*RLBTRP         .
BRLCTRP         .
BRLDTRP         .
BRD1L           .
BRD2L           .
BRD3L           .
BRD4L           .
BRD5L           .
BRD6L           .
BRD7L           .
BRD8L           .
BRGA+GB         .
BRD1H           .
BRD2H           .
BRD3H           .
BRD4H           .
BRD5H           .
BRD6H           .
BRD7H           .
*  MAJOR STATUS CHANGE CONFIGURATIONS IN CRUISE AFFECT THESE
BRLC            .                                                    X
                                                                     X

  L1.L2.L3.^SL.^L4
BRLC            .                                                    X
                                                                     X

  L1.L2.^SL.^L4
BRLCZ3          .                                                    X
                                                                     X

  L1.L2.L3.SL.^L4
BRLCZ3          .                                                    X
                                                                     X

  L1.L2.SL.^L4
BRLD            .                                                    X
                                                                     X

  L1.L2.L3.^SL.^L4
```

```
BRLD          .                                                          X
                                                                         X

  L1.L2.^SL.^L4
BRLDZ3        .                                                          X
                                                                         X

  L1.L2.L3.SL.^L4
BRLDZ3        .                                                          X
                                                                         X

  L1.L2.SL.^L4
BRLA          .                                                          X
                                                                         X

  L1.L2.L3.^SL.^L4
BRLA          .                                                          X
                                                                         X

  L1.L2.^SL.^L4
BRLAZ3        .                                                          X
                                                                         X

  L1.L2.L3.SL.^L4
BRLAZ3        .                                                          X
                                                                         X

  L1.L2.SL.^L4
*RLB          .                                                          X
*                                                                        X
* L1.L2.L3.^SL.^L4
*RLB          .                                                          X
*                                                                        X
* L1.L2.^SL.^L4
*RLBZ3        .                                                          X
*                                                                        X
* L1.L2.L3.SL.^L4
*RLBZ3        .                                                          X
*                                                                        X
* L1.L2.SL.^L4
BRTAN         .                                                          X
                                                                         X

  W1.W2.D3.^D8.^GA.^GB
BRTAN         .                                                          X
                                                                         X

  W1.W2.^D8.^GA.^GB
BRTLO         .
BRTLO         .                                                          X
                                                                         X

  W1.W2.D5.^D6.^GA.^GB.^UT
BRTHI         .
BRTHI         .                                                          X
                                                                         X

  W1.W2.D7.^D8.^GA.^GB.^UT


DATA_RECORD_SYNTAX:  See the Description of Data segment of the
DATA_SET_PARAMETER section.
Each record has terminators of the \n form.

/* EOF */
```